FRA-78-8

REPORT NO. FRA/ORD 75/96

EVALUATION OF PROTOTYPE HEAD SHIELD FOR HAZARDOUS MATERIAL TANK CAR

Milton R. Johnson

IIT RESEARCH INSTITUTE
10 West 35th Street
Chicago IL 60616

DECEMBER 1976

FINAL REPORT

Prepared for

U.S. DEPARTMENT OF TRANSPORTATION
FEDERAL RAILROAD ADMINISTRATION
Office of Research and Development
Washington DC 20591

NOTICE

This document is disseminated under the sponsorship of the Department of Transportation in the interest of information exchange. The United States Government assumes no liability for its contents or use thereof.

NOTICE

The United States Government does not endorse products or manufacturers. Trade or manufacturers' names appear herein solely because they are considered essential to the object of this report.

Technical Report Documentation Page

1. Report No.	2. Government Accession No.	3. Recipient's Catalog No.
FRA/ORD 75/96		

4. Title and Subtitle	5. Report Date
EVALUATION OF PROTOTYPE HEAD SHIELD FOR HAZARDOUS MATERIAL TANK CAR	December 1976
	6. Performing Organization Code
7. Author(s)	8. Performing Organization Report No.
Milton R. Johnson	DOT-TSC-FRA-76-8
9. Performing Organization Name and Address	10. Work Unit No. (TRAIS)
IIT Research Institute* 10 West 35th Street Chicago IL 60616	RR628/R7323
	11. Contract or Grant No.
	DOT-TSC-727
12. Sponsoring Agency Name and Address	13. Type of Report and Period Covered
U.S. Department of Transportation Federal Railroad Administration Office of Research and Development Washington DC 20591	Final Report Sept. 1974-Apr. 1975
	14. Sponsoring Agency Code

15. Supplementary Notes

*Under contract to: U.S. Department of Transportation
Transportation Systems Center
Kendall Square
Cambridge MA 02142

16. Abstract

The structural integrity of a prototype tank car head shield for hazardous material railroad tank cars was evaluated under conditions of freight car coupling at moderate to high speeds. This is one of the most severe environments encountered in normal railroad service. Two versions of the shield were tested. They were installed on a DOT Spec. 112A340W tank car and instrumented to measure forces at the points of attachment between the shield and the car. Test data were obtained when the car was impacted into standing cars over a 3 to 9 mph speed range. The tests produced no visible damage to the shield or the structure connecting it to the tank car, but they demonstrated the presence of severe vibrations resulting from the car impact. The likelihood of fatigue damage was indicated in the connecting structural members where the weight of the shield was supported. Modifications to the supporting structure are recommended before proceeding with additional impact tests and over-the-road tests.

17. Key Words	18. Distribution Statement
Tank Cars, Tank Car Head Shields, Tank Car Hazards, Freight Car Impact	DOCUMENT IS AVAILABLE TO THE U.S. PUBLIC THROUGH THE NATIONAL TECHNICAL INFORMATION SERVICE, SPRINGFIELD, VIRGINIA 22161

19. Security Classif. (of this report)	20. Security Classif. (of this page)	21. No. of Pages	22. Price
Unclassified	Unclassified	60	

Form DOT F 1700.7 (8-72)

Reproduction of completed page authorized

PREFACE

The work described in this report was conducted by IIT Research Institute (IITRI) under the authorization of Transportation Systems Center (TSC) Contract DOT-TSC-727, Amendment No. 5.

This report presents results of the evaluation of the structural integrity of a prototype tank car head shield when exposed to certain conditions representative of the normal railroad service environment. This project is one facet of the Federal Railroad Administration (FRA) Tank Car Safety Program. The prototype shield utilized in the test was designed by Louisiana Tech University (LTU), under the direction of Dr. Mike Wilkinson. The evaluation tests described in this report were carried out at the Research and Development Division of Miner Enterprises, Inc., Chicago, under the direction of Mr. Robert Arseneau. The shield was installed on a car provided to the FRA through arrangements with the Railway Progress Institute/Association of American Railroads (RPI/AAR) Tank Car Safety Project.

The IITRI Project Manager for this work was Dr. M. R. Johnson. Mr. E. Scharres and Mr. Glenn Kutzer of IITRI's Experimental Operations Section assisted in the recording and analysis of the data. Mr. P. Cannon of IITRI's Digital Systems Group processed that portion of the data requiring computer analysis. Mr. William Hathaway was the cognizant TSC Technical Monitor. His helpful suggestions and guidance throughout the course of the work is gratefully acknowledged.

METRIC CONVERSION FACTORS

Approximate Conversions to Metric Measures

Symbol	When You Know	Multiply by	To Find	Symbol
		LENGTH		
in	inches	2.5	centimeters	cm
ft	feet	30	centimeters	cm
yd	yards	0.9	meters	m
mi	miles	1.6	kilometers	km
		AREA		
in^2	square inches	6.5	square centimeters	cm^2
ft^2	square feet	0.09	square meters	m^2
yd^2	square yards	0.8	square meters	m^2
mi^2	square miles	2.6	square kilometers	km^2
	acres	0.4	hectares	ha
		MASS (weight)		
oz	ounces	28	grams	g
lb	pounds	0.45	kilograms	kg
	short tons (2000 lb)	0.9	tonnes	t
		VOLUME		
tsp	teaspoons	5	milliliters	ml
Tbsp	tablespoons	15	milliliters	ml
fl oz	fluid ounces	30	milliliters	ml
c	cups	0.24	liters	l
pt	pints	0.47	liters	l
qt	quarts	0.95	liters	l
gal	gallons	3.8	liters	l
ft^3	cubic feet	0.03	cubic meters	m^3
yd^3	cubic yards	0.76	cubic meters	m^3
		TEMPERATURE (exact)		
°F	Fahrenheit temperature	5/9 (after subtracting 32)	Celsius temperature	°C

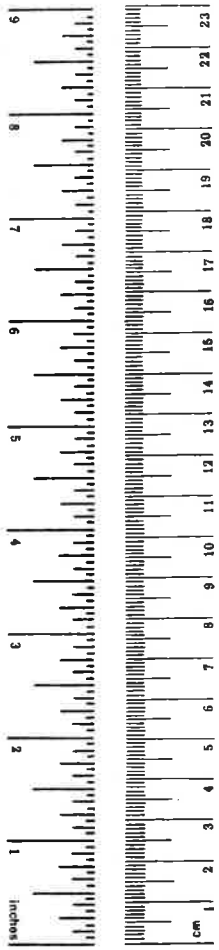

Approximate Conversions from Metric Measures

Symbol	When You Know	Multiply by	To Find	Symbol
		LENGTH		
mm	millimeters	0.04	inches	in
cm	centimeters	0.4	inches	in
m	meters	3.3	feet	ft
m	meters	1.1	yards	yd
km	kilometers	0.6	miles	mi
		AREA		
cm^2	square centimeters	0.16	square inches	in^2
m^2	square meters	1.2	square yards	yd^2
km^2	square kilometers	0.4	square miles	mi^2
ha	hectares (10,000 m^2)	2.5	acres	
		MASS (weight)		
g	grams	0.035	ounces	oz
kg	kilograms	2.2	pounds	lb
t	tonnes (1000 kg)	1.1	short tons	
		VOLUME		
ml	milliliters	0.03	fluid ounces	fl oz
l	liters	2.1	pints	pt
l	liters	1.06	quarts	qt
l	liters	0.26	gallons	gal
m^3	cubic meters	35	cubic feet	ft^3
m^3	cubic meters	1.3	cubic yards	yd^3
		TEMPERATURE (exact)		
°C	Celsius temperature	9/5 (then add 32)	Fahrenheit temperature	°F

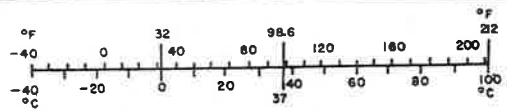

TABLE OF CONTENTS

LIST OF ILLUSTRATIONS

LIST OF ILLUSTRATIONS (CONT)

1. INTRODUCTION

This report presents interim results in the evaluation of a prototype head shield for hazardous material tank cars with respect to the maintenance of its structural integrity under normal service loads. It deals with the behavior of the shield under car coupling impacts which is one of the most severe environments. Subsequent investigations will evaluate the performance of the shield under other aspects of the load environment. The evaluation of the shield's ability to reduce the probability of head puncture in the accident environment is not within the scope of this program.

1.1 BACKGROUND

The program to evaluate a prototype head shield is in support of the FRA/TSC program dealing with the application of tank car head shields for protection against puncture. The principal hazard occurs in derailments when cars separate and couplers of adjacent cars may be forced against the tank heads causing their rupture and the subsequent release of hazardous materials. The addition of a head protection shield at the ends of cars carrying hazardous gases under pressure is expected to be an effective means of reducing such punctures. However, in order to retain their effectiveness and to avoid causing an accident themselves, the protective shields must remain fixed securely to the cars throughout their expected lifetimes.

The overall purpose of this program is to determine the reliability against fatigue damage of one or more prototype head protection shields. Fatigue damage of the tank shell or of the structural components of the car to which the shield is attached, may develop during normal service operations resulting in damage to the basic car structure or to the shield. If significant fatigue damage should occur there is the possibility of a separation of the shield from the car.

Under FRA authorization, Louisiana Tech University (LTU) has had the responsibility to develop prototype head protection shield designs and select one or more of these designs for fabrication. The goal of this program is to determine the safety margin of these specific designs against fatigue failure so that the reliability of the system can be projected over the service life of the car.

The evaluation of the head shield involves three general tasks:

- definition of the load spectra describing the environment of the shield attachment to a tank car,
- determination, both by analytical and experimental means, of the fatigue damage sensitivity of one or more prototype head shield designs including the calculation and verification of service life expectancy,
- establishment of guidelines for securing high-integrity long-life attachment of head shields to tank cars.

This report deals with the results of a preliminary investigation of one aspect of the definition of the load environment, namely, the behavior of the shield under car impact conditions.

1.2 CHARACTERISTICS OF LTU SHIELD

The basic principle which is followed in the LTU shield design is to avoid direct attachment to the tank head and minimize load transfer to the stub sill. The weight of the shield is supported by a structural member which spans the width of the car between the side sills. This member also rests on the stub sill, which therefore supports some of the weight of the shield. The upper portion of the shield is held in position by two supporting members, one on each side of the car, which connect the sides of the shield with the tank car bolster. Two different designs of this member have been tested, one providing more flexibility than the other in the longitudinal direction.

Figures 1 and 2 show the version of the shield design which utilizes a strap side support between the shield and the tank car bolster. The strap provides substantial flexibility in the longitudinal direction. Figure 2 shows a detailed view of the strap and of the angle which spans the width of the car and provides vertical support for the shield. Figure 3 shows the version of the shield design which utilizes a tube support member between the shield and the tank car bolster. This design provides a more rigid connection in the longtiduinal direction. A detailed view of the method of connecting the angle to the side sills is shown in Figure 4. This figure also illustrates the support given by the stub sill to this angle at the center of the car. There is a shim between the stub sill and the support angle which is not visible in the photograph. Initially a gap was left between the angle and the stub sill to accommodate a load cell for the measurement of vertical loads. When this measurement technique proved to be impractical a shim was inserted to support the angle. The angle rests on the shim and is not directly connected to the shim or the stub sill.

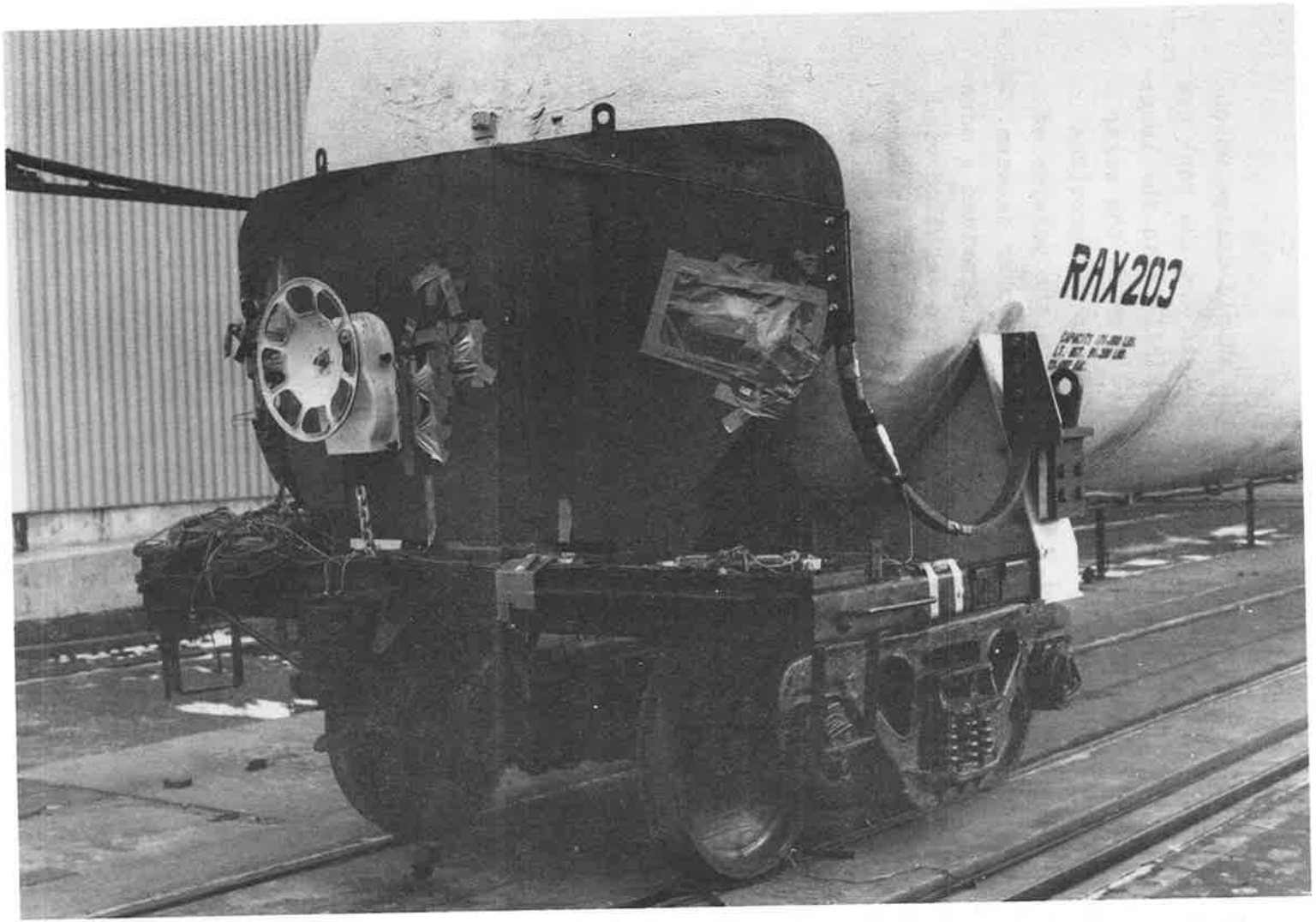

Figure 1. SHIELD WITH STRAP CONNECTION TO BOLSTER

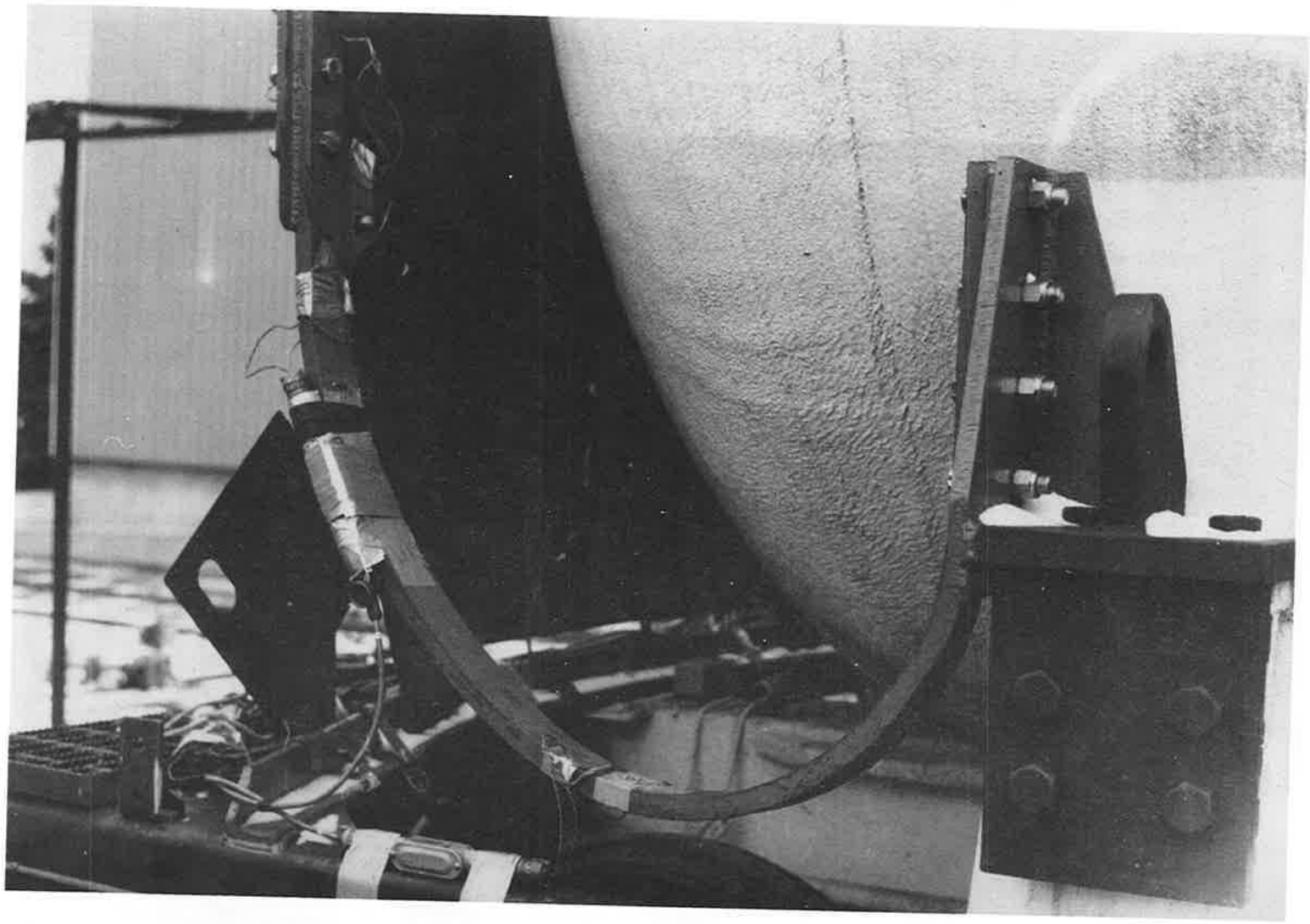

Figure 2. DETAIL OF STRAP AND ANGLE SUPPORT

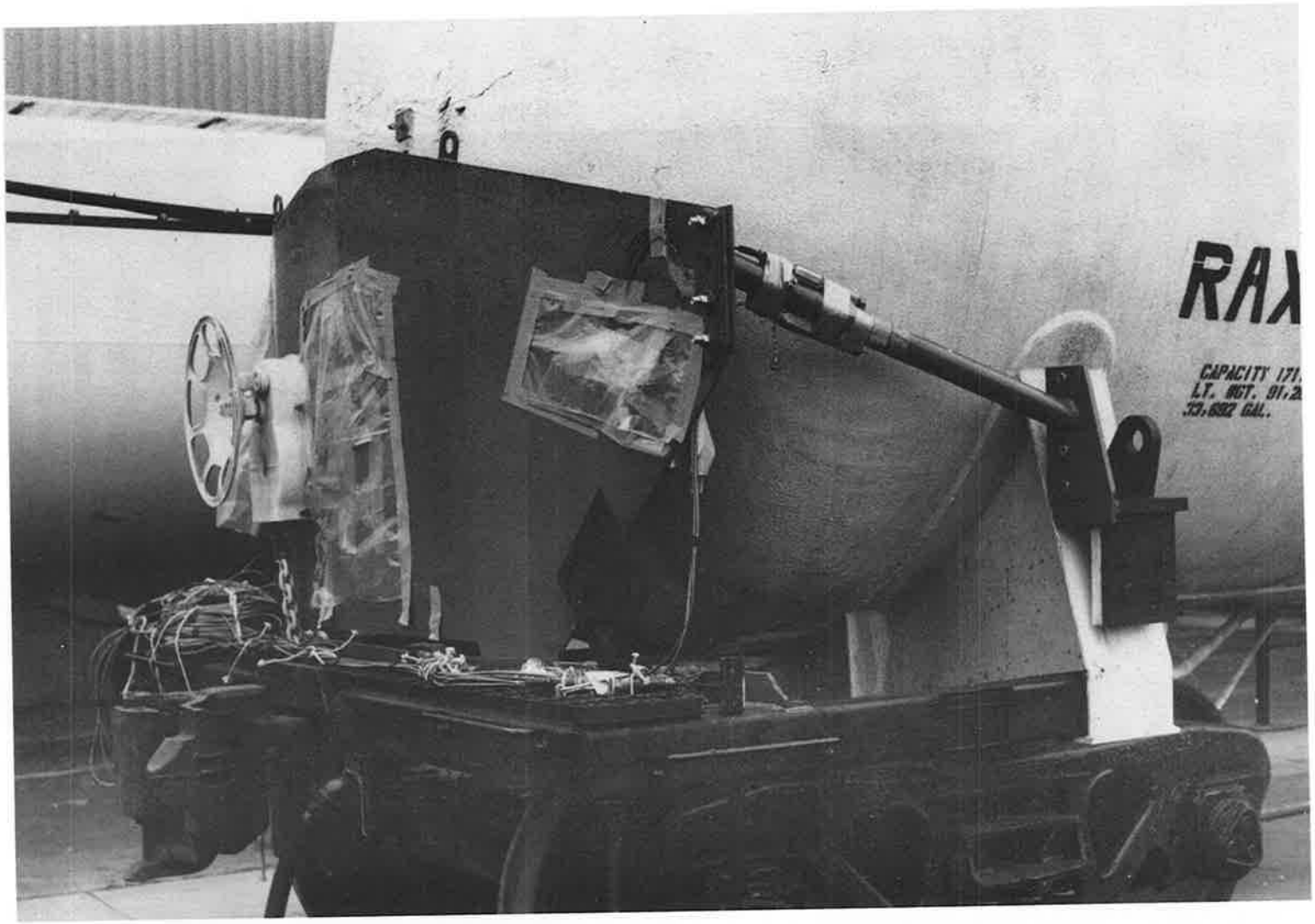

Figure 3. SHIELD WITH TUBE CONNECTION TO BOLSTER

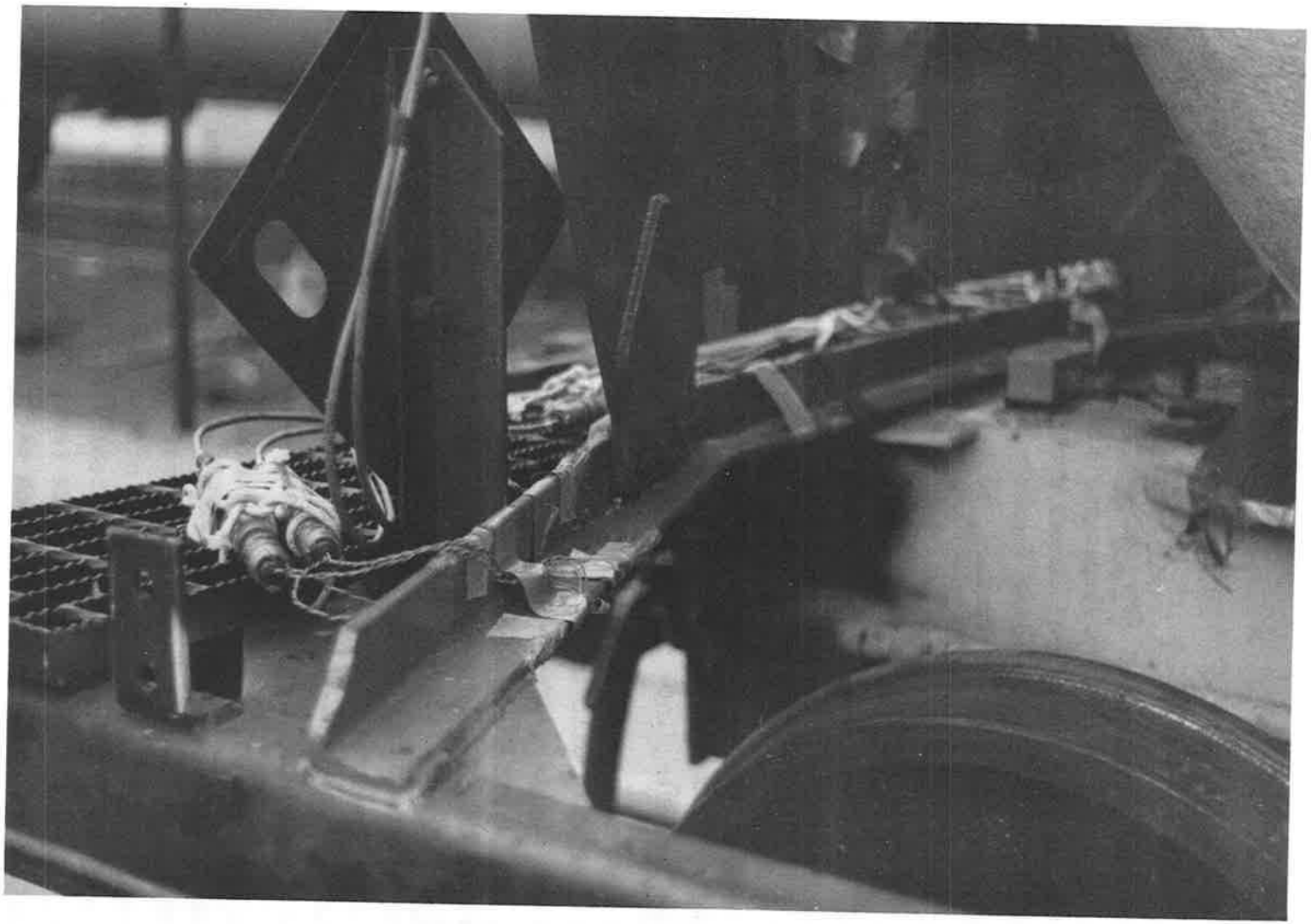

Figure 4. DETAIL OF ANGLE SUPPORT CONNECTION TO SIDE SILL

2. TEST PLAN

A preliminary review of the head shield design indicated that one of the most severe load environments would be the inertial loads accompanying sudden accelerations of the car on which the shield is mounted. Therefore, it was decided that the behavior of the shield under car coupling impact conditions would be the first aspect of the load environment to be evaluated.

2.1 TEST PROCEDURES

Two types of car impact tests were planned and conducted. The shield was installed on the hammer car for the first tests. This type of test is illustrated in Figure 5a and is subsequently referred to as the "hammer car" test. Under these conditions the primary load acting on the shield is a longitudinal inertial load which results from a sudden deceleration of the car when it is stopped by impacting into the standing cars.

The prototype head shield was installed on a 33,000 gallon capacity tank car built in conformance to DOT specification 112A340W for non-insulated pressure tank cars. The car, designated RAX 203, had an empty weight of 91,200 lbs and an allowable loaded rail load of 263,000 lbs. It was equipped with a draft gear conforming to AAR specification M-901E. The shield and tank car were instrumented with transducers to provide a continuous output of strain, accelerations, loads, etc. The shield was installed on the B-end (hand-brake end) of the car which was positioned so that the head shield was on the leading (striking) end of the car.

The tank car was impacted into three standing 100 ton capacity hopper cars. Each car was loaded with sand to a 220,000 lb rail load. These cars were equipped with draft gear conforming to AAR specification M-901. The hand-brakes of the standing cars were applied and track skates were placed behind one set of wheels on each car. It was recognized that this resulted in more severe resisting forces to the impacting tank car than free standing cars, but the test setup represented an upper limit to the severity of the conditions that can be found in service and allowed close control in the repeatability of test conditions.

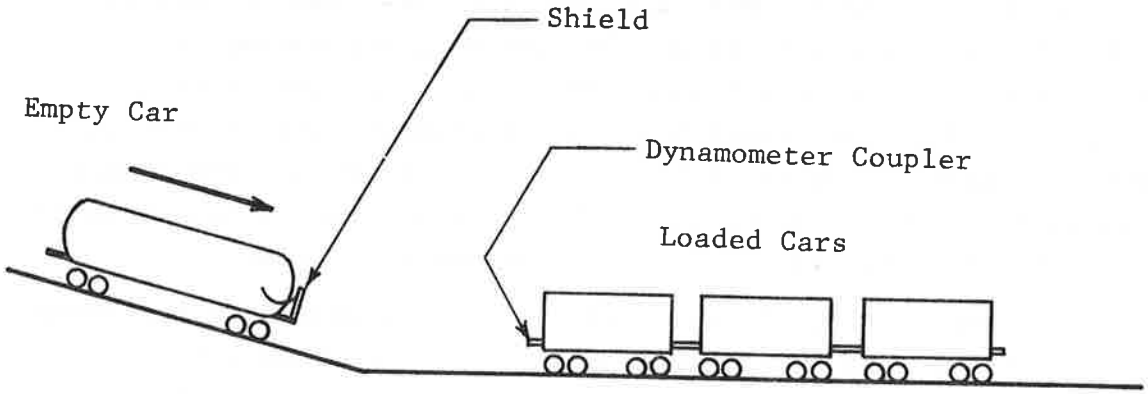

(a) Hammer Car Test

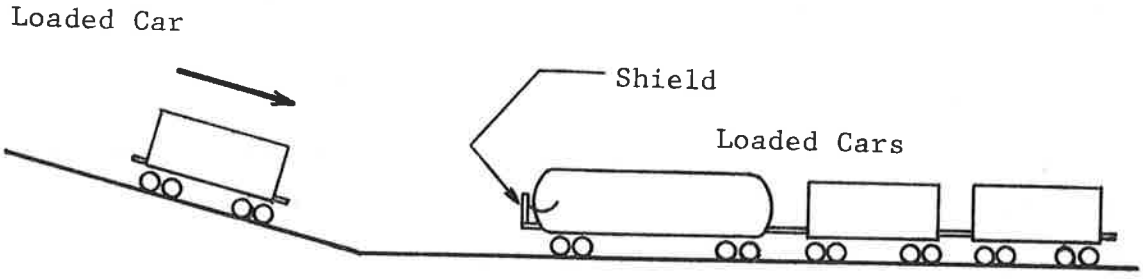

(b) Anvil Car Test

Figure 5. ARRANGEMENT OF CARS FOR IMPACT TESTS

The tank car was empty for the hammer car tests. This condition results in more severe car decelerations than testing with a loaded car. The car was accelerated to predetermined velocities by releasing it on an inclined ramp. The first impact test was conducted at approximately 3 mph and subsequent impact velocities were increased in approximately 3/4 mph increments. The impact velocities were increased until the force limitation (approximately 1,200,000 lbs) was reached in the dynamometer coupler.

The second type of test used for the evaluation of the prototype tank car head shields was conducted in accordance with Paragraph 24-5 of the AAR Tank Car Specifications. This test is specified as a method of evaluating head shield design in the Federal Regulation which requires head shields on hazardous material tank cars. The test is conducted by impacting a loaded car into a standing tank car equipped with the head shield as illustrated in Figure 5b. This test procedure is subsequently referred to as the "anvil car" test.

2.2 INSTRUMENTATION

The instrumentation was configured to develop the following information:

- the magnitude of the forces transmitted to the car from the shield,
- the vibrational response of the shield to the impact,
- strain levels within the shield.

The transducers used to develop the data are described in the following paragraphs. The locations of the transducers are shown in Figures 6 through 10. The specific characteristics of the transducers are listed in Appendix A.

Accelerometers (Figure 6) mounted on the plate of the shield were used to determine the vibrational modes in the head shield structure. Accelerometers (Figure 6) mounted on the stub sill were used to determine rigid body motions of the car.

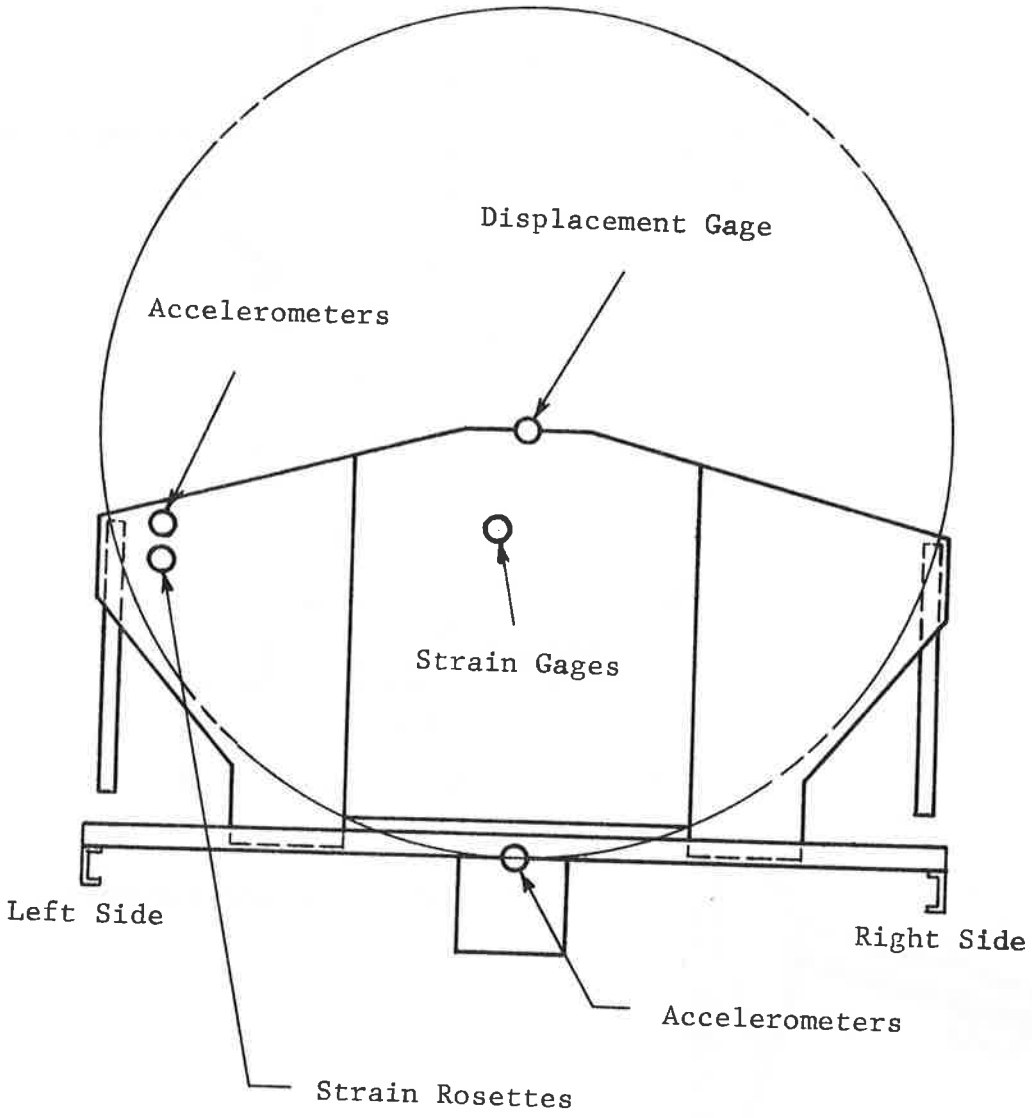

Figure 6. TRANSDUCER LOCATIONS, FRONT VIEW OF SHIELD

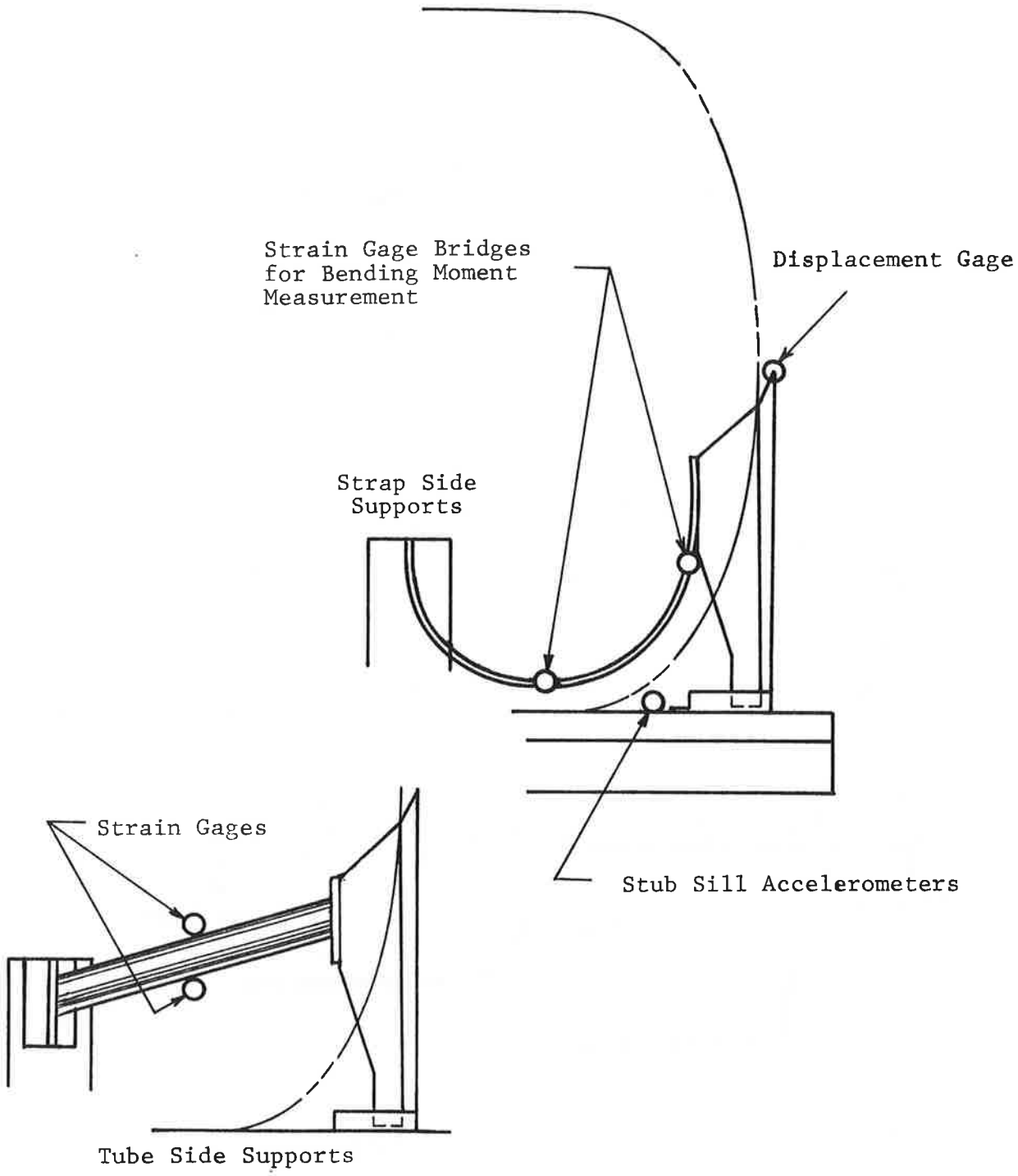

Figure 7. TRANSDUCER LOCATIONS, SIDE VIEW OF SHIELD AND CAR

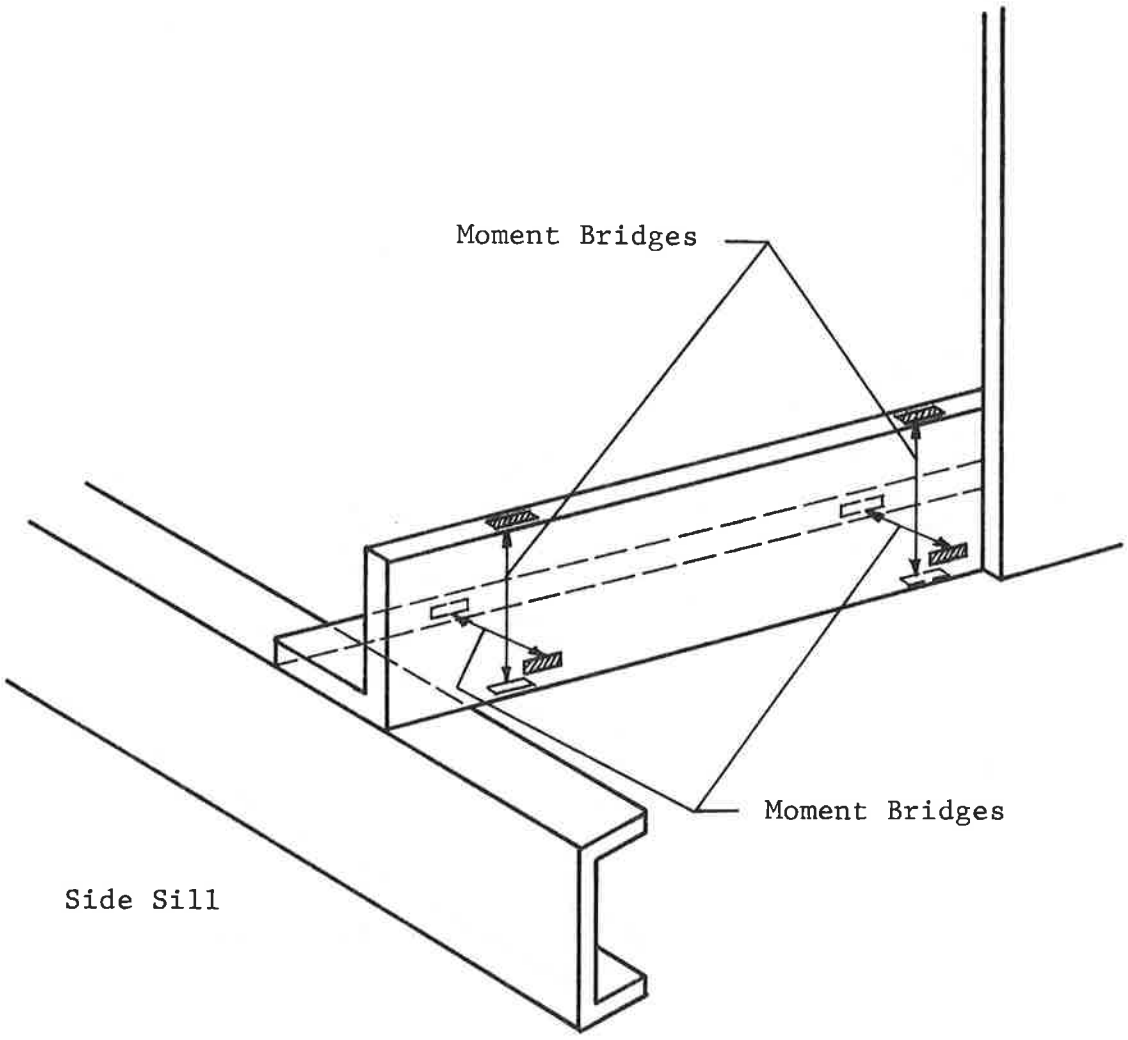

Figure 8. STRAIN GAGE PLACEMENT ON HEAD SHIELD SUPPORT ANGLE, LEFT SIDE OF CAR

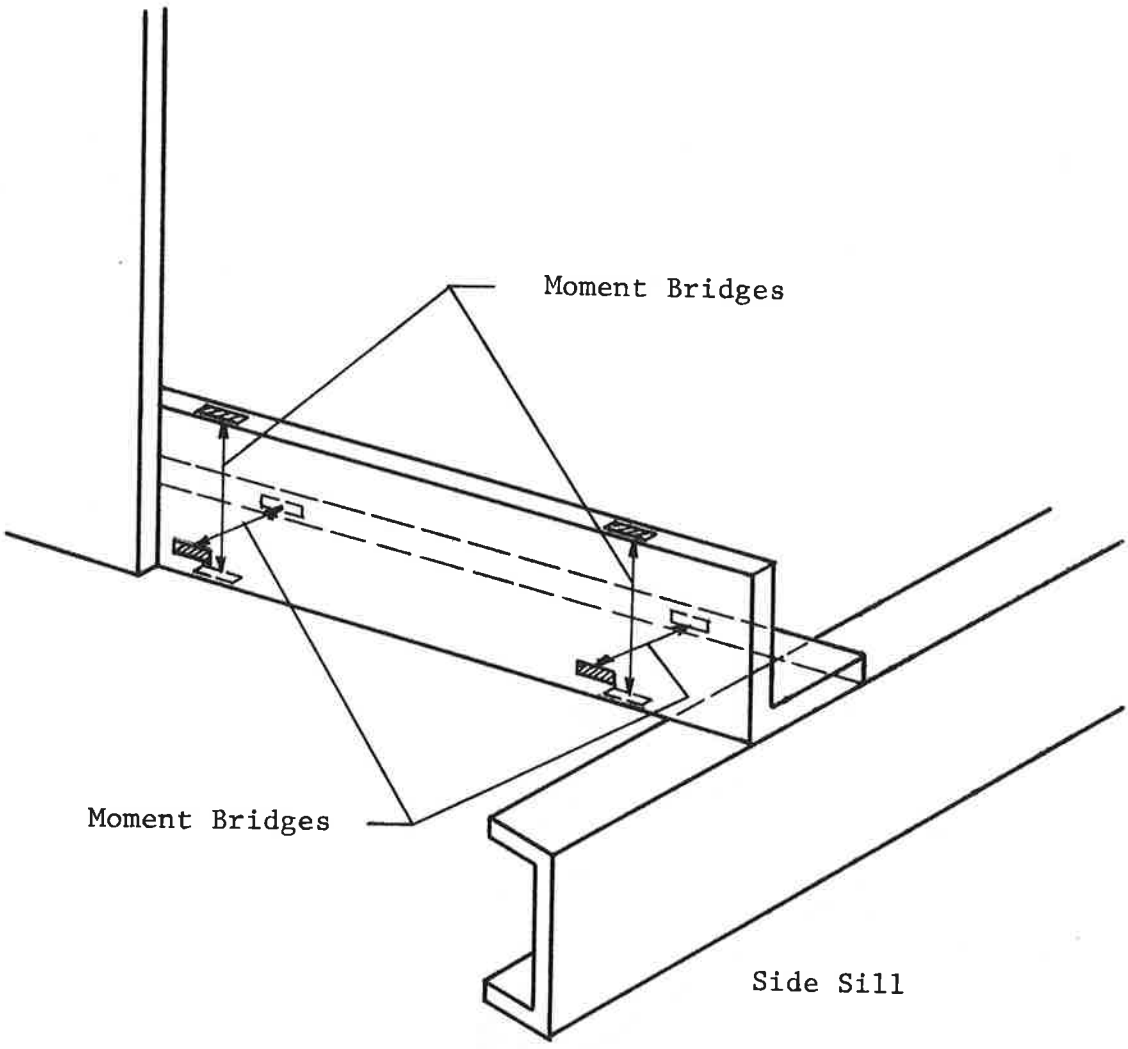

Figure 9. STRAIN GAGE PLACEMENT ON HEAD SHIELD SUPPORT ANGLE, RIGHT SIDE OF CAR

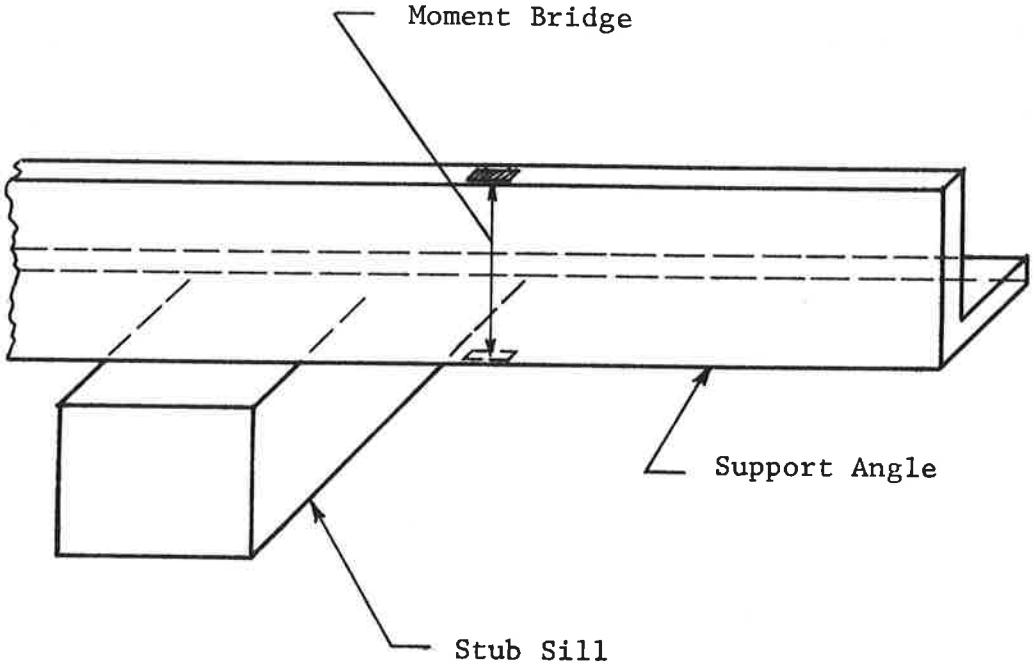

Figure 10. STRAIN GAGE PLACEMENT ON HEAD SHIELD SUPPORT ANGLE NEAR CENTER OF CAR

Strain rosettes (Figure 6) were used to determine the stress field in the plate adjacent to the side support connections. The data from these gages were also used to identify principal vibrational frequencies. Additional strain gages, oriented horizontally, were placed on the front and back side of the plate near the center of the shield (Figure 6).

Strain gages (Figure 7) mounted on the side supports were used to determine the longitudinal inertial loads transmitted to the car structure through these elements. When the strap side supports were used strain gages wired into bending bridges were placed at two elevations as shown in Figure 7. The magnitude and elevation of the longitudinal load could be estimated from the two sets of moment data. Strain gages were mounted in only one position when using the rigid tube side supports and the outputs of these gages were recorded independently. This data provided an estimate of the longitudinal load through the tube and the elevation of its line-of-action.

Strain gages were mounted on the support angle between the side sill and the shield attachment to determine the bending moments in the angle in both the horizontal and vertical planes parallel to the member (Figures 8 and 9). By knowing the differences in the bending moments between the two sets of gages it is possible to calculate the vertical and horizontal components of shear in the member and thus define the interfacial loads between the support angle and the side sill. Strain gages were also mounted on the support angle adjacent to the stub sill (Figure 10) to estimate the bending moment in the vertical plane and thus indicate the vertical load transfer to the stub sill by this member.

Movement of the shield with respect to the car was monitored by a displacement gage (Figure 6) between the top of the shield and the tank head. A dynamometer coupler was used in the anvil car to provide a record of coupler force as a function of time during the impact.

High speed motion pictures were also taken. On two of the tests one camera, operating at approximately 500 fps, was positioned to obtain a side-on view of the shield. On all tests three cameras, operating at 64 fps were positioned to obtain additional data on the behavior of the shield.

The data was recorded on magnetic tape at 7.5 ins./sec. Two recorders were used for this purpose. The recorders were located within the Miner instrumentation facility adjacent to the test track. These recorders were connected to the transducers on the tank car through a 1500 ft long hard-wire system. The cables are hung from trolleys adjacent to the test track so that they can follow the movement of the car.

2.3 TEST OPERATIONS

Four series of impact tests were performed: two test series with the strap (flexible) side supports and one with the tube (rigid) side supports utilizing the hammer car test procedure, and one test series with the strap support system utilizing the anvil car test procedure.

The first test was performed on November 5, 1974 utilizing the hammer car test procedure and the strap side supports. The impact speeds and associated maximum coupler forces are tabulated as follows:

Impact Velocity (mph)	Maximum Coupler Force (1000 lbs)
3.25	NR*
3.94	NR
4.55	NR
5.24	NR
5.80	479
6.84	680
7.26	908
7.94	1051
8.51	1177
9.25	1303

*NR: not recorded.

The second test series was performed on November 13, 1974 utilizing the hammer car test procedure and the tube side supports. The impact speeds and associated maximum coupler forces are tabulated as follows:

Impact Velocity (mph)	Maximum Coupler Force (1000 lbs)
3.00	166
3.90	288
4.74	403
5.48	505
6.31	628
7.21	765
8.06	1140
8.86	1380

The third impact series was performed on December 17, 1974. It was a repeat of the conditions utilized on the first test. The test was repeated because during the analysis of the data it was discovered that some of the transducers did not produce the required information. Also, there was an indication of severe loading of the horizontal member supporting the shield and it was desired to verify this data. The impact speeds and associated maximum coupler forces are tabulated as follows:

Impact Velocity (mph)	Coupler Force (1000 lbs)
2.96	223
3.84	300
4.68	430
5.48	440
6.29	694
7.20	905
7.98	1260
8.02	1260

The fourth impact test series was performed on February 4, 1975 utilizing the anvil car test procedure and the strap side supports for the shield. The impact speeds and associated maximum coupler forces are tabulated as follows:

Impact Velocity (mph)	Coupler Force (1000 lbs)
3.94	325
5.98	650
7.04	1200
7.36	1300

3. TEST RESULTS

The results from the first three impact test series (hammer car tests) showed that the stresses within the shield itself and the loads within the side supports were within acceptable limits, but that the angle which supported the weight of the shield was highly stressed. The high angle stresses were due to the excitation of vertical vibratory motions. As expected, the dynamic response of the shield with the strap supports was greater than the shield with the tube supports. The results from the fourth test series (the anvil car test) showed unexpectedly high loads in the supporting structure of the shield which were due in part to the dynamic response sensitivity of the shield to the displacement of the tank car as it is struck by the impacting car. The test data are compared and described in the following subsections.

3.1 COMPARISON OF HAMMER CAR TEST DATA

This section compares data from the hammer car tests of November 13th (tube side supports) and December 17th (strap side supports).

3.1.1 Shield Displacement

Figure 11 compares the maximum longitudinal displacement of the top of the shield as a function of impact velocity for both methods of shield connection to the bolster. As expected, the strap support allows approximately twice the deflection of the shield as the tube support. The frequencies for the fundamental longitudinal mode of vibration were 4.8 Hz when the strap supports were used and 10.1 Hz when the tube supports were used.

3.1.2 Strains in Shield Plate

The greater flexibility provided by the strap support results in lower strains in the shield itself. This is shown by the data presented in Figures 12 and 13. Figure 12 compares maximum horizontal strains measured at the center of the shield for the two versions of the support system as a function of impact velocity.

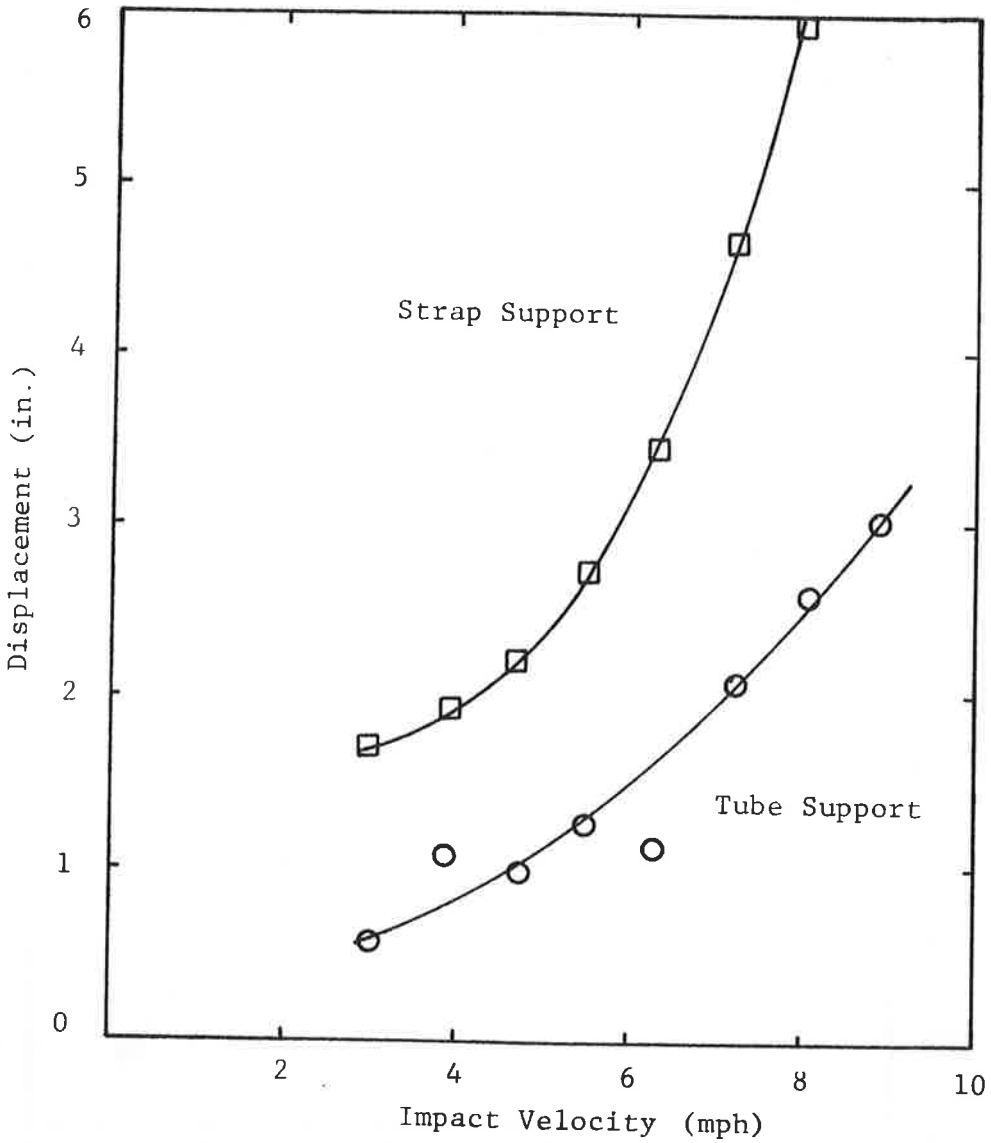

Figure 11. MAXIMUM LONGITUDINAL DISPLACEMENT (AWAY FROM CAR) OF TOP CENTER OF SHIELD

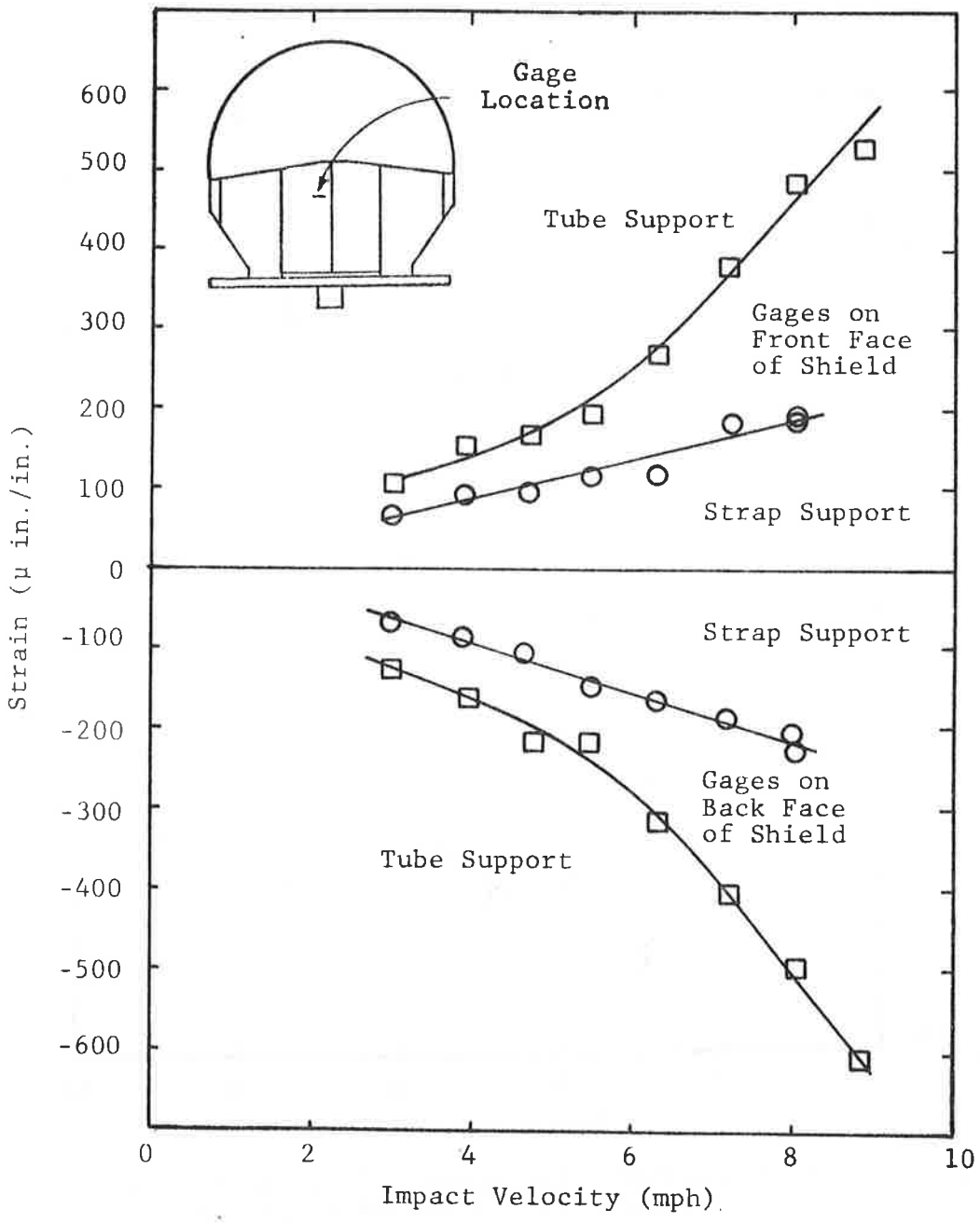

Figure 12. MAXIMUM HORIZONTAL STRAINS MEASURED ON GAGES AT CENTER OF SHIELD

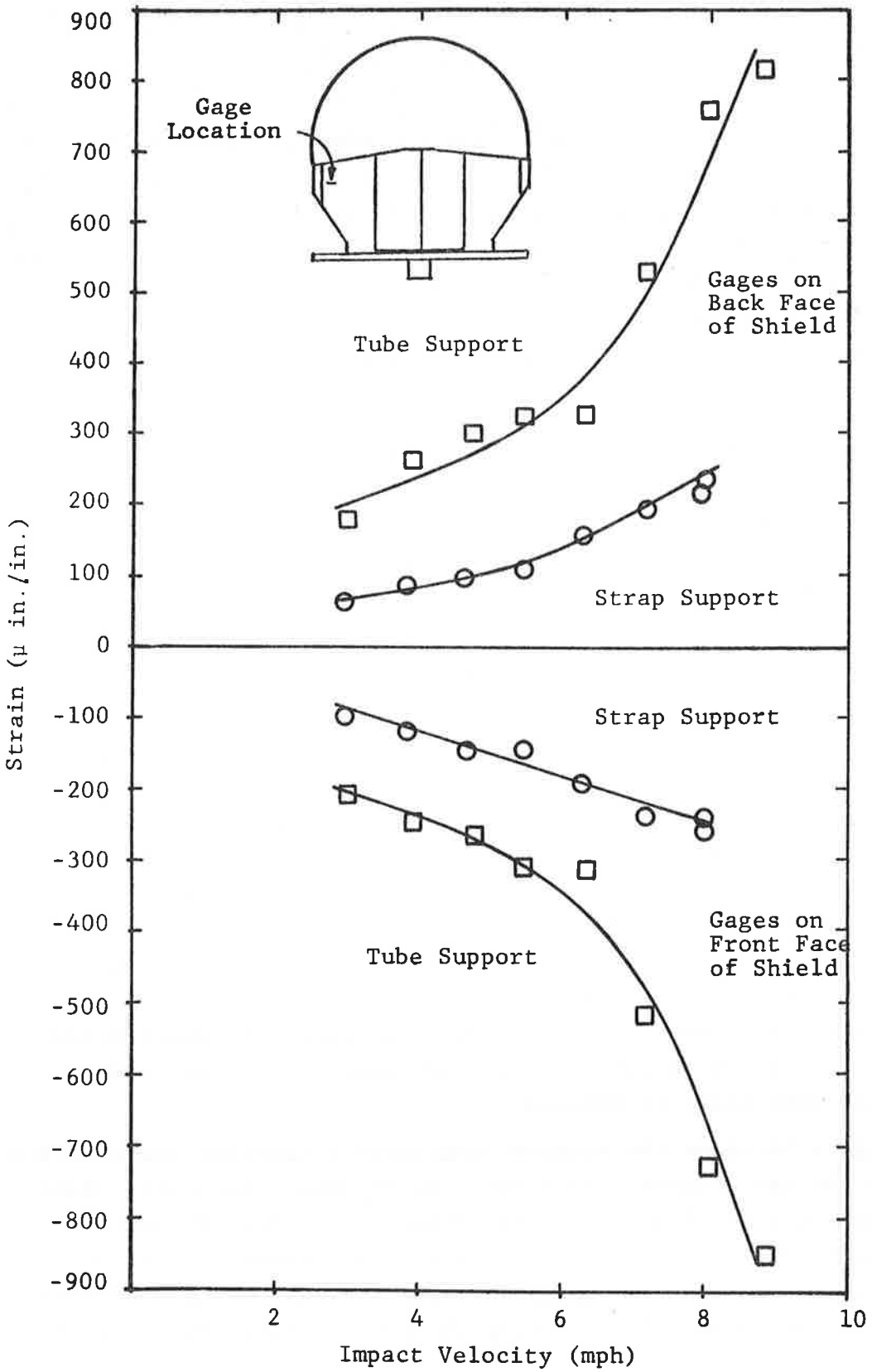

Figure 13. MAXIMUM HORIZONTAL STRAINS MEASURED ON LEFT SIDE OF SHIELD

Note that all strains are well below the elastic limit of the material (approximately 1,300μ in./in.) and that the strains with the strap support are approximately one-half of those with the tube support. Figure 13 makes a similar comparison of horizontal strains measured at the left hand side of the shield. Again it will be noted that the strains are below the elastic limit and that they are significantly higher with the tube support system.

3.1.3 Forces Transmitted Through the Side Supports

The magnitude and character of the inertial forces transmitted from the shield to the car structure are of particular interest to the evaluation of the shield structural system. There are two paths for these loads: through the side support structure and through the horizontal support angle. We discuss first the loads transmitted through the side supports.

The data presented in Figures 14 through 16 show the magnitude of the maximum transient loads exerted on the tank car bolster through both the strap and tube side support systems. Figure 14 shows the maximum longitudinal load acting through the strap supports as a function of impact velocity. Note that these inertial loads are higher on the left side of the car (facing the shield) where the hand brake is located. The distance above the base of the shield of the line-of-action of this load is shown in Figure 15 as a function of impact velocity. These distances are approximately constant over the range of impact velocities. The line-of-action is slightly lower on the left side where the hand brake is located.

Figure 16 shows the maximum longitudinal inertial loads acting through the tube supports as a function of impact velocity. Note that the loads are from two to six times higher than the corresponding loads transmitted through the strap supports. This data is not as accurate as the strap load data because of the low strain levels in the tubes. It is estimated that the data presented in

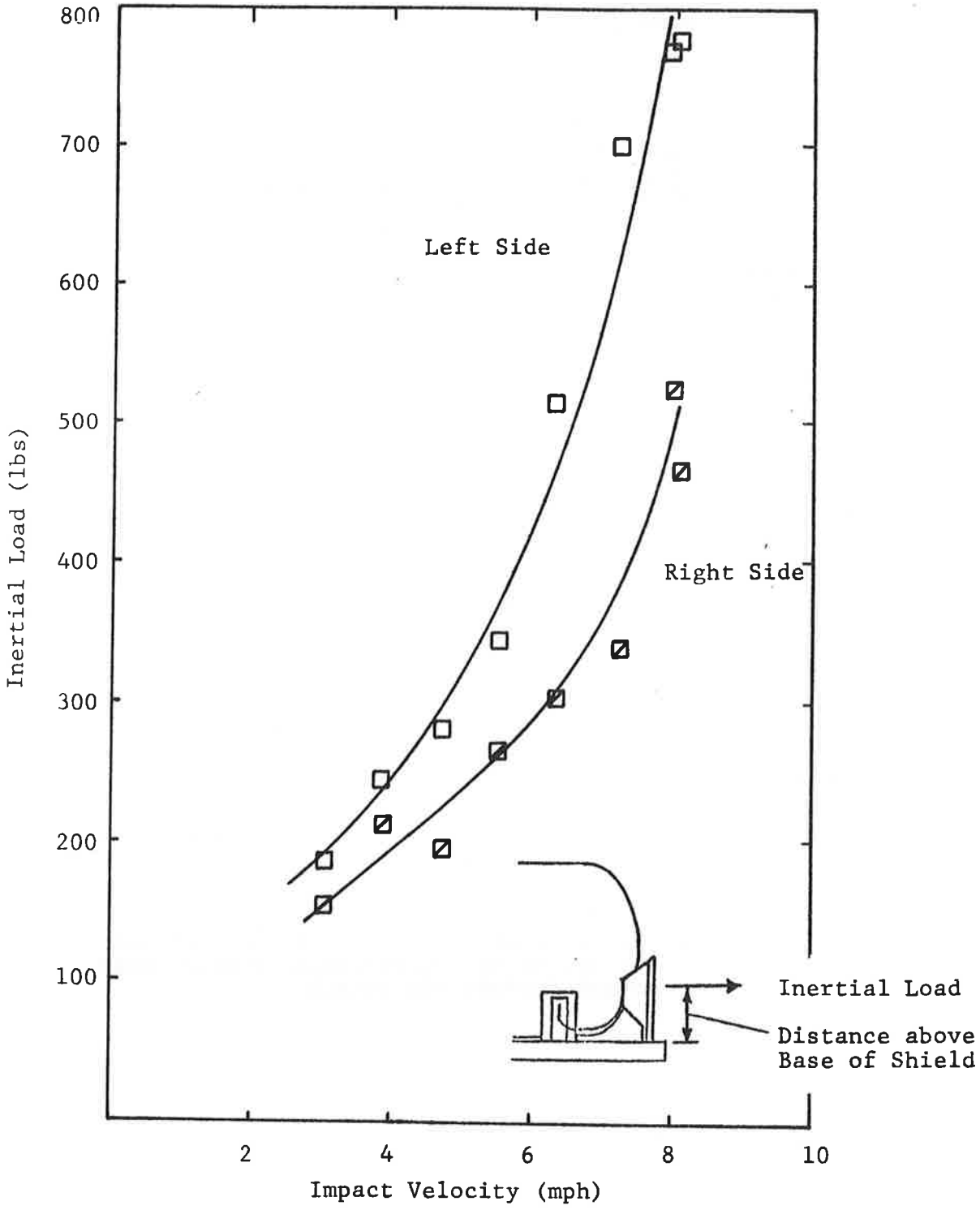

Figure 14. MAXIMUM LONGITUDINAL INERTIAL LOAD ACTING THROUGH STRAP SHIELD SUPPORTS

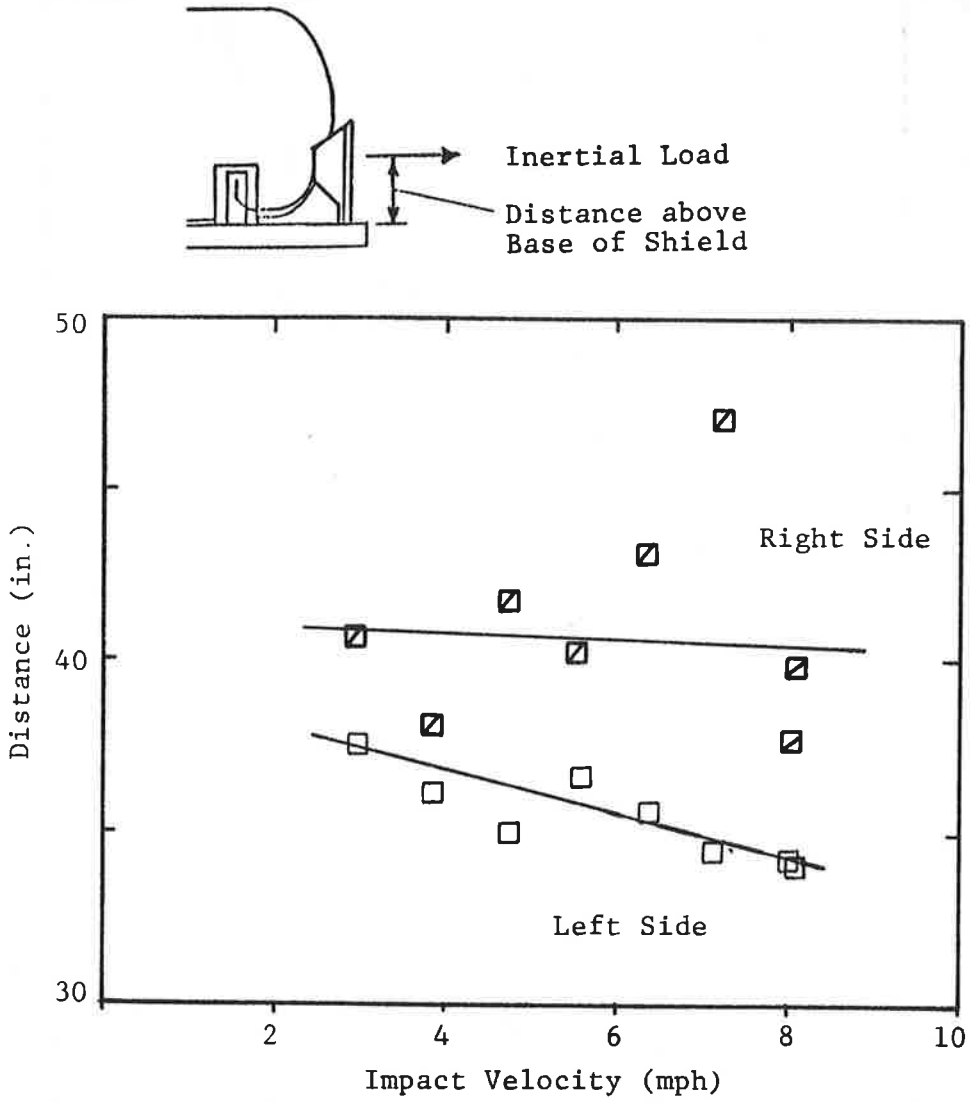

Figure 15. DISTANCE ABOVE BASE OF SHIELD FOR LINE-OF-ACTION OF LONGITUDINAL INERTIAL LOAD, STRAP SUPPORT FOR SHIELD

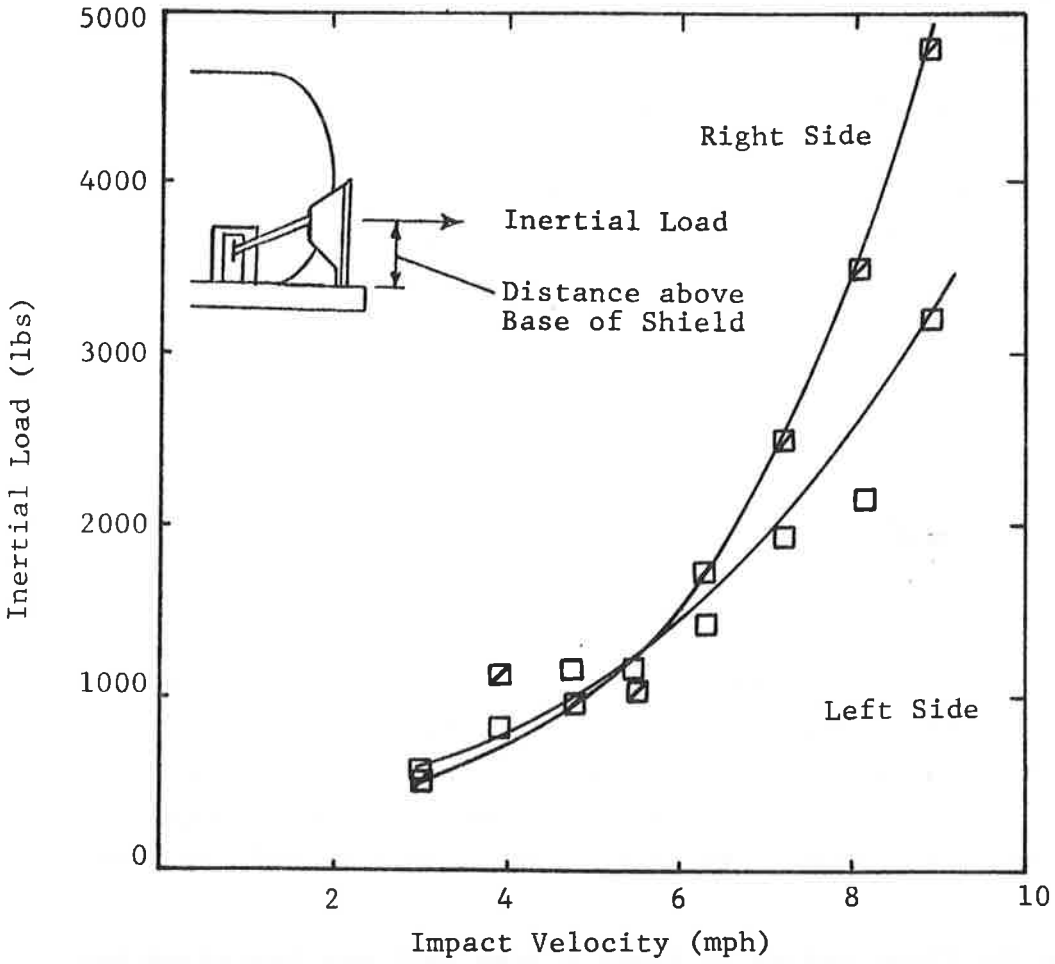

Figure 16. MAXIMUM LONGITUDINAL INERTIAL LOAD ACTING THROUGH TUBE SHIELD SUPPORTS

Figure 16 is within 25 percent of the true values. The distance of the line-of-action of the longitudinal load above the base of the shield with the tube supports was determined to be approximately 35 inches over the range of impact velocities. The capacity of the tank car bolster to withstand the longitudinal loads from the shield side supports has been calculated to be in excess of 10,000 lbs so that the maximum forces from either the tube or strap side supports are within acceptable limits.

3.1.4 Forces Transmitted Through the Support Angle

The second path of load transfer between the shield and car is through the horizontal angle which supports the weight of the shield. As previously stated, this angle is welded to the side sills and rests on the stub sill so that the loads are transferred into the structure of the car at these points.

Load transfer through this member under car impact conditions involves complex response phenomena. The primary load would be expected to be a longitudinal inertial load, although some vertical excitation would not be unexpected. A longitudinal inertial load acting on the angle at the shield supports would be reacted both by axial tensile and shear forces in the angle. The axial tensile forces would be due to the fact that the outer portions of the angle are bent with respect to a transverse reference line. The shear forces would be due to the rigid connections at the side-sill/angle and shield/angle interfaces and would result from bending of the angle. Vertical loads carried through this member would be transmitted both to the stub sill and the side sills.

On the first series of tests a load cell was installed between the angle and the stub sill in an attempt to measure load transfer at this position, if any. Load transfer to the side sills through shear in the angle was measured by installing two sets of bending bridges between the shield attachment and the side sill (see Figures 8 and 9). These sets of gages permitted the determination of moments on the principal axes of the angles at two

locations, thus allowing for the calculation of shear forces. These shear forces were resolved into longitudinal and vertical components.

The tests revealed that under car impact the longitudinal displacement of the shield is coupled into a vertical motion which displaces the support angle in a vertical direction. This motion was most pronounced with the strap side supports. The angle was lifted off the stub sill and impacted against it during the downward phase of the motion. There was less vertical motion developed with the tube side supports, but the lifting of the angle off the stub sill was still observed during the higher velocity impacts.

This phenomena damaged the load cell placed between the angle and the stub sill on the first test series making it impossible to measure the loads transferred at this position. The stresses within the angle measured by the bending bridges were substantial. On the first series of tests the yield point of several gages was exceeded at impact velocities above 7 mph. On the second and third test series there was no apparent yielding indicated by the gages.

Figures 17 through 22 show the results of a computer analysis of the data from the two sets of bending bridges on the right side of the car for the second and third test series. This data permits comparison of the use of the rigid and flexible side supports. These figures show plots of the vertical and longitudinal shear loads as a function of time, which are transferred through the angle and act on the side sill for the third, fifth and seventh impact tests of each series. These data were obtained by processing the analog data on a Nova 1220 mini-computer. The procedure included digitizing the signal from each bending bridge, performing transformations to determine the moments about the principal axes, computing the shear loads with respect to the principal axes, and combining the longitudinal and vertical components of the shear loads.

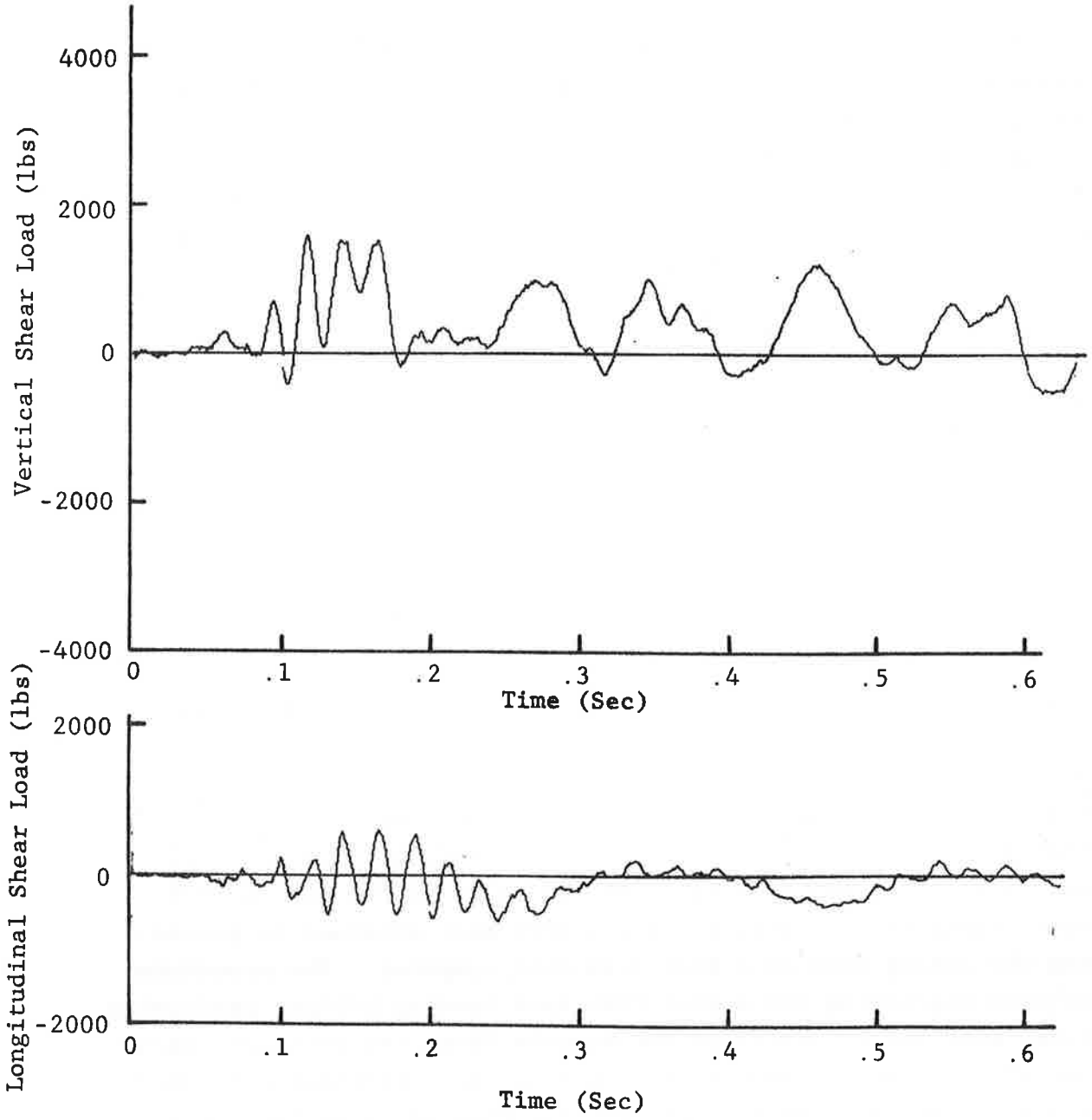

Figure 17. VERTICAL AND LONGITUDINAL SHEAR LOADS ON SIDE SILL FROM SHIELD SUPPORT ANGLE, FLEXIBLE STRAP SUPPORT, IMPACT NO. 3, 4.68 MPH (NOTE: POSITIVE LOAD IS DOWN OR FORWARD)

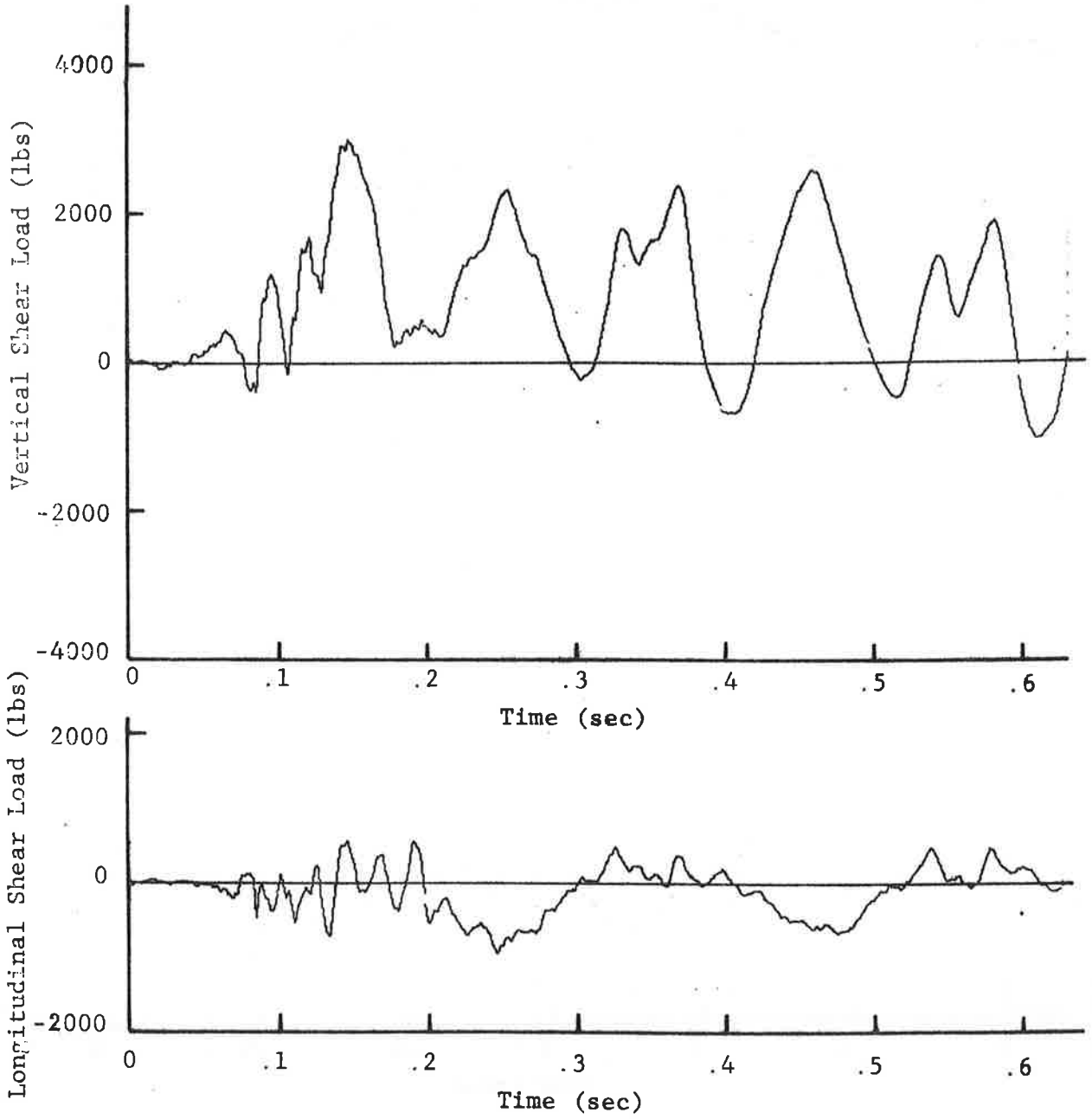

Figure 18. VERTICAL AND LONGITUDINAL SHEAR LOADS ON SIDE SILL FROM SHIELD SUPPORT ANGLE, FLEXIBLE STRAP SUPPORT, IMPACT NO. 5, 6.29 MPH (NOTE: POSITIVE LOAD IS DOWN OR FORWARD)

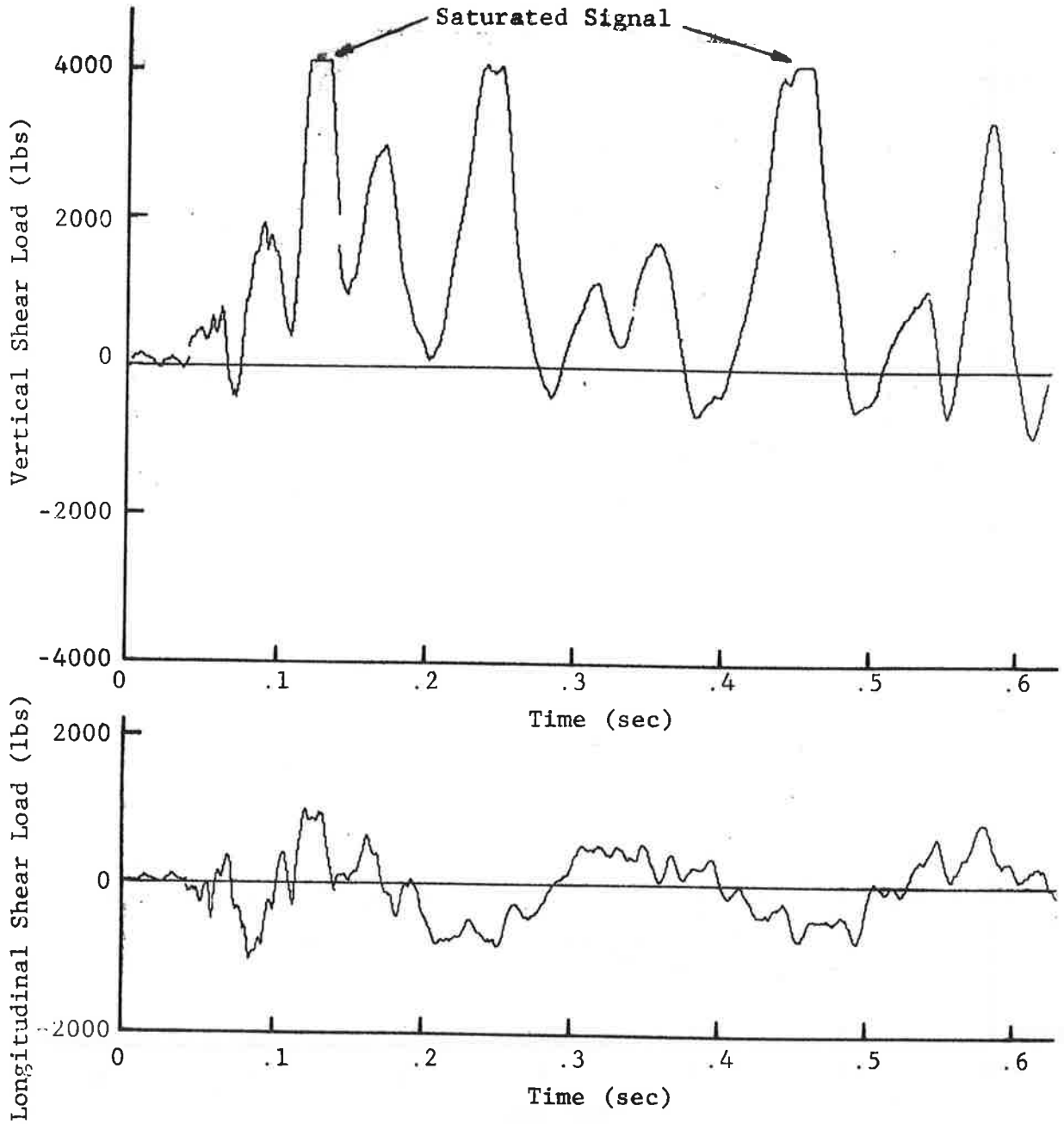

Figure 19. VERTICAL AND LONGITUDINAL SHEAR LOADS ON SIDE SILL FROM SHIELD SUPPORT ANGLE, FLEXIBLE STRAP SUPPORT, IMPACT NO. 7, 7.98 MPH (NOTE: POSITIVE LOAD IS DOWN OR FORWARD)

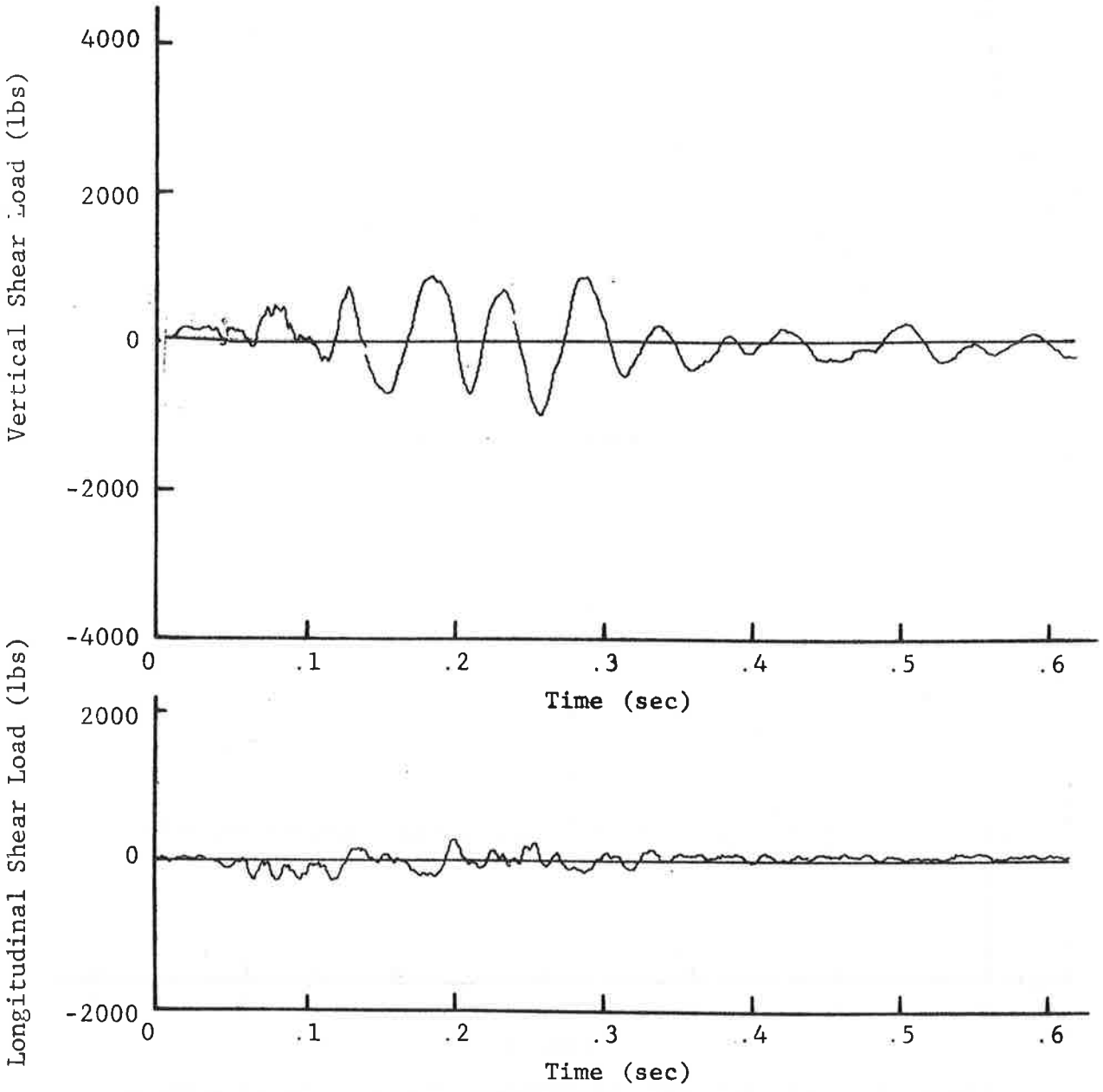

Figure 20. VERTICAL AND LONGITUDINAL SHEAR LOADS ON SIDE SILL FROM SHIELD SUPPORT ANGLE, RIGID TUBE SUPPORT, IMPACT NO. 3, 4.74 MPH (NOTE: POSITIVE LOAD IS DOWN OR FORWARD)

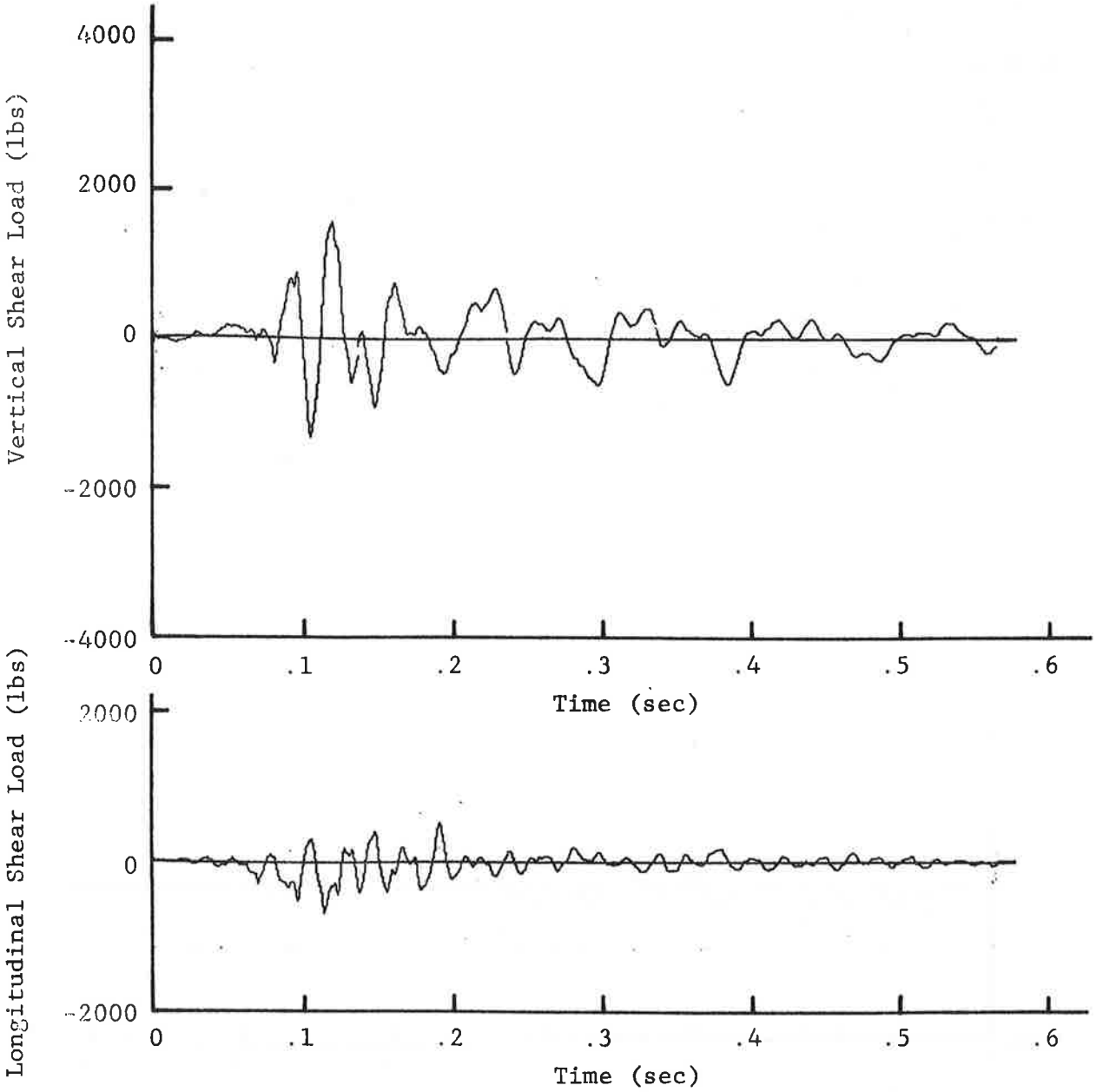

Figure 21. VERTICAL AND LONGITUDINAL SHEAR LOADS ON SIDE SILL FROM SHIELD SUPPORT ANGLE, RIGID TUBE SUPPORT, IMPACT NO. 5, 6.31 MPH (NOTE: POSITIVE LOAD IS DOWN OR FORWARD)

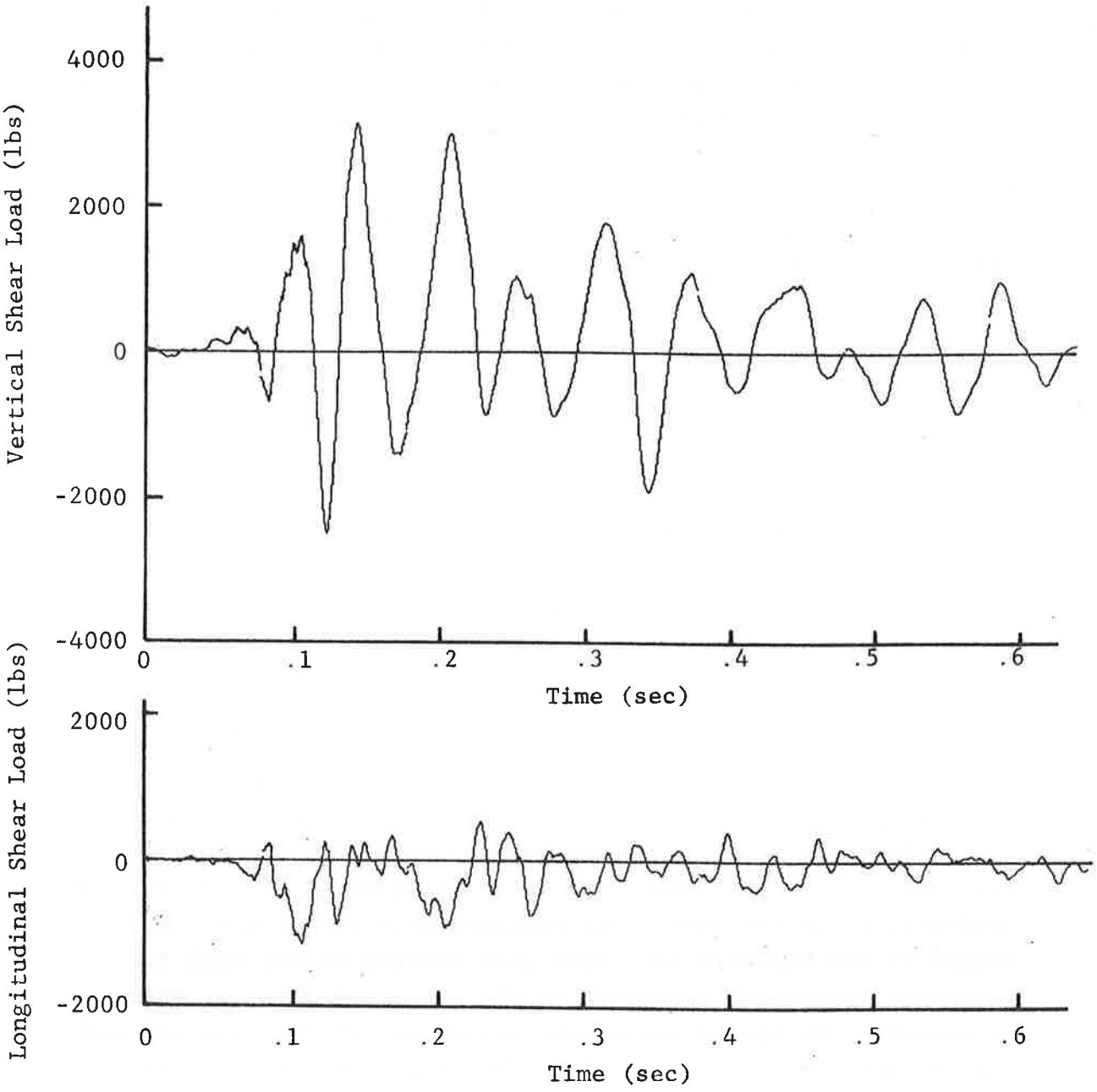

Figure 22. VERTICAL AND LONGITUDINAL SHEAR LOADS ON SIDE SILL FROM SHIELD SUPPORT ANGLE, RIGID TUBE SUPPORT, IMPACT NO. 7, 8.06 MPH (NOTE: POSITIVE LOAD IS DOWN OR FORWARD)

Figures 17 through 19 show the vertical and longitudinal shear loads associated with the use of flexible strap side supports. Note that in each case the vertical load component rapidly grows in magnitude into a complex waveform which exceeds the magnitude of the longitudinal shear load. The fundamental frequency of the vertical shear load is approximately 10 Hz although the presence of higher frequency components is evident. The longitudinal waveform shows the fundamental 4.8 Hz vibration associated with the longitudinal shield vibration. A higher frequency component, approximately 40 Hz, is apparent through the first cycle of the longitudinal shear load, but this has decayed substantially after .2 sec. Note the high vertical shear loads associated with the 7.98 mph impact. These loads are associated with the vertical impacting of the angle against the stub sill.

Figures 20 through 22 show similar data associated with the use of rigid tube side supports. Note that the peak magnitudes are lower. The lower levels of shear load are in agreement with the observation of reduced vertical vibration of the shield with the rigid tube side supports. Table 1 summarizes the longitudinal and vertical shear load data for all of the impact tests of the second and third series.

3.2 ANVIL CAR TESTS

The anvil car impact tests, which were conducted in accordance with Paragraph 24-5 in the AAR Tank Car Specifications, involved impacting a fully loaded 70 ton capacity (nominal) car, (referred to as the hammer car) into the standing loaded tank car (referred to as the anvil car) equipped with the shield. Two loaded 70 ton capacity cars were also coupled to the tank car providing additional restraint to the motion of this car when it is struck. The shield was at the struck end of the tank car and was equipped with the strap (flexible) supports for this test.

Initially it was believed that this test would be less severe than the hammer car tests. The tests revealed, however, that the maximum loads on the shield and the supporting structure were

TABLE 1. MAXIMUM SHEAR LOADS ON RIGHT SIDE SILL FROM SUPPORT ANGLE FOR IMPACT TESTS WITH FLEXIBLE AND RIGID SIDE SUPPORTS

	Impact Velocity (mph)	Maximum Shear Load on Side Sill			
		Vertical (lbs)		Longitudinal (lbs)	
		Down	Up	Forward	Backward
Flexible Strap Side Supports	3.00	900	500	500	200
	3.90	1100	300	800	300
	4.74	1600	400	700	500
	5.48	2100	600	500	700
	6.31	3000	900	600	900
	7.21	4000+	900	1200	1100
	8.06	4000+	1000	1000	1000
	8.86	4000+	700	1000	1200
Rigid Tube Side Supports	2.96	400	300	100	0
	3.84	400	300	100	0
	4.68	800	1000	300	200
	5.48	1000	900	200	300
	6.29	1600	1300	600	700
	7.20	1800	1500	500	700
	7.98	3200	2400	600	1100
	8.02	3900	2900	800	1300

somewhat higher than on the hammer car tests. Figure 23 compares the maximum displacement between the end of the tank and the top of the shield for the two types of tests. The maximum displacement always occurred at the first peak for the hammer car tests. With the anvil car test the second peak was somewhat higher than the first peak.

The large displacements and strains measured on the anvil car tests were somewhat surprising in view of the fact that the shield equipped car is initially at rest and that it is displaced a relatively short distance, on the order of 6 to 30 inches, from the effects of the impact by the hammer car.

A detailed study of the motions of the struck car suggests that the start-stop motion, which is imparted to the car by the impact, is in phase with the fundamental mode of longitudinal oscillation of the shield and that this tends to amplify the shield displacement. Figure 24 shows the displacement of the struck car as a function of time in both the longitudinal and vertical directions. This data was derived from motion pictures taken of the impact. Note that in addition to the longitudinal motion there is a smaller vertical motion of the car which is on the order of 5 Hz. Figure 25 shows the longitudinal velocity of the struck car as a function of time. The sharp rise and fall in the velocity within the first .1 sec could be the reason that the dynamic response of the fundamental mode (4.8 Hz) of the shield is amplified after the first peak.

The amplification of response phenomena following the first peak is also noted in Figures 26 and 27 when comparing strain data from the center and left side of the shield for the two types of tests. Strain data from the center of the shield, Figure 26, show the first peak of the anvil car test is below comparable data from the hammer car test, but that the second peak is substantially higher. Strain data from the left side of the shield, Figure 27, show that the first peak of the anvil car test is approximately the same as comparable data from the hammer car tests, and that the second peak is slightly higher.

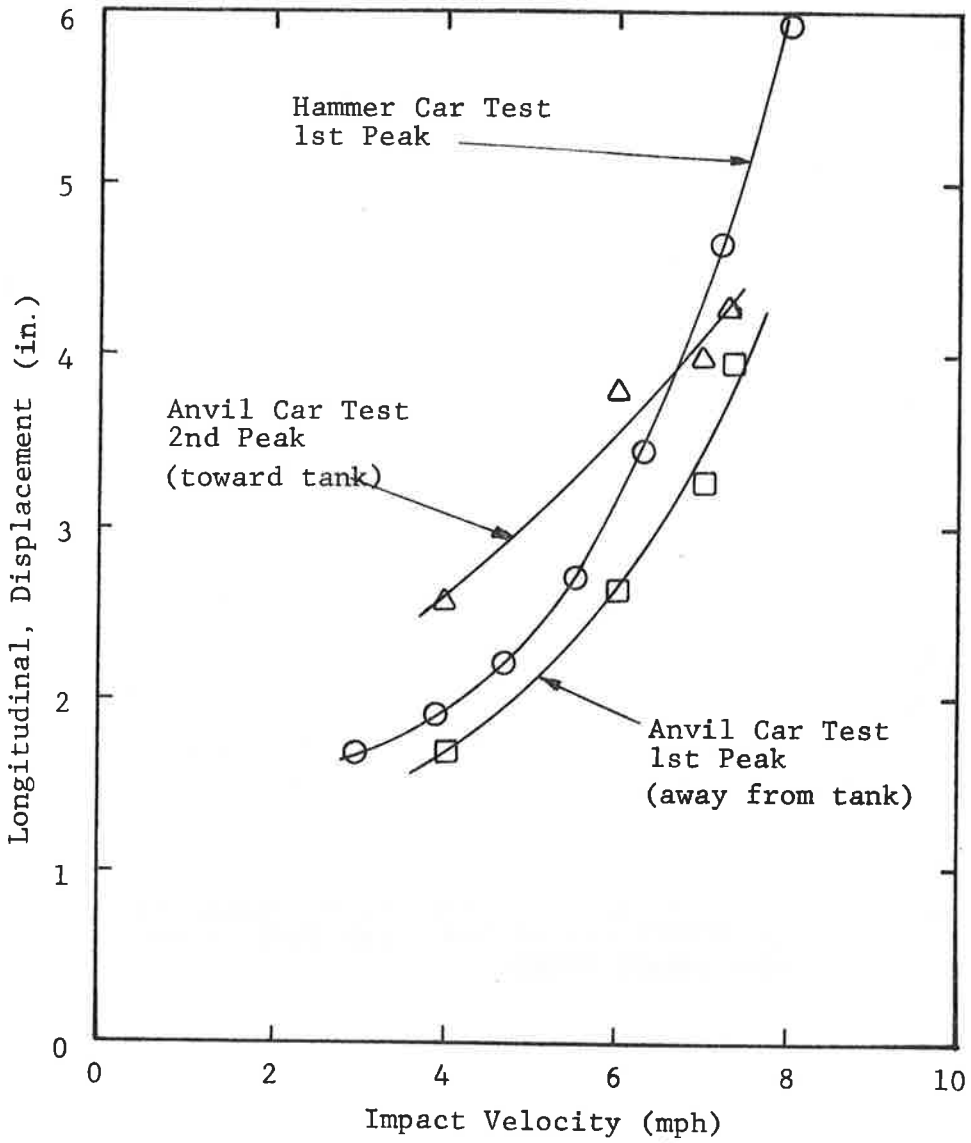

Figure 23. LONGITUDINAL DISPLACEMENT (AWAY FROM CAR) OF TOP CENTER OF SHIELD, COMPARISON OF HAMMER CAR AND ANVIL CAR TEST DATA

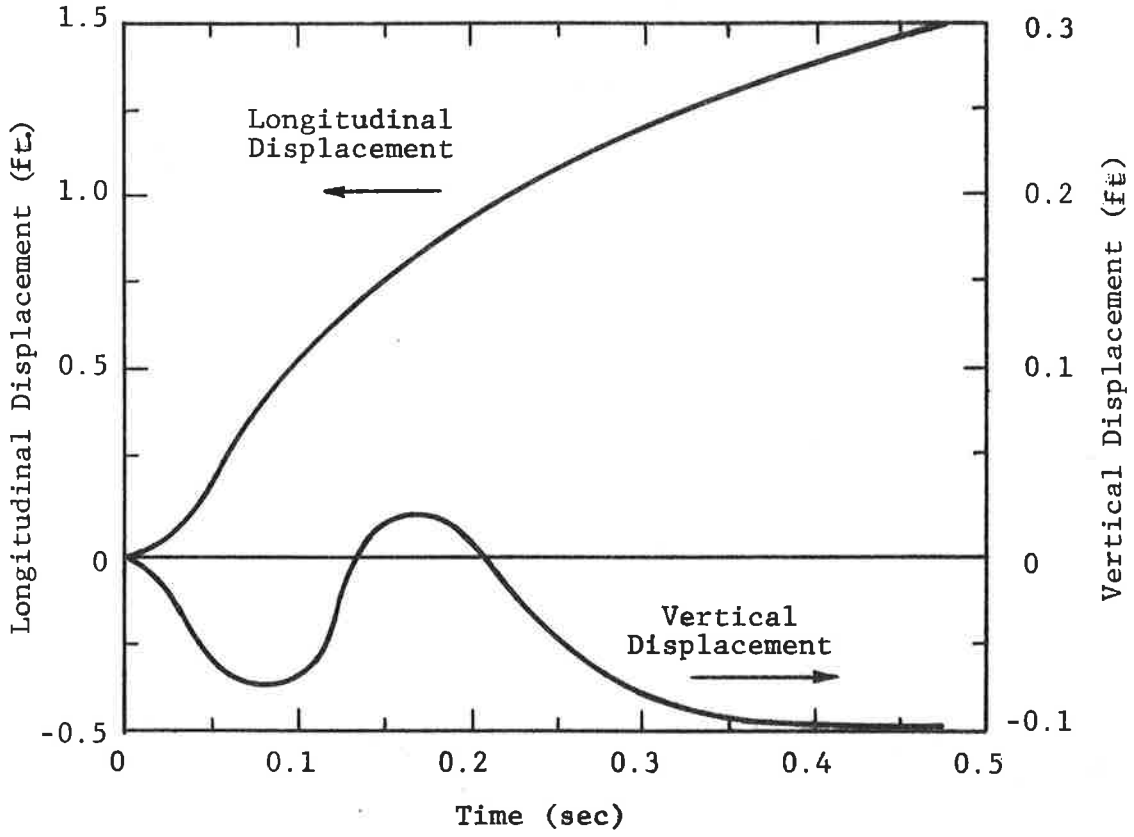

Figure 24. LONGITUDINAL AND VERTICAL DISPLACEMENT OF STRUCK CAR ON ANVIL CAR TEST, 7.04 MPH IMPACT SPEED

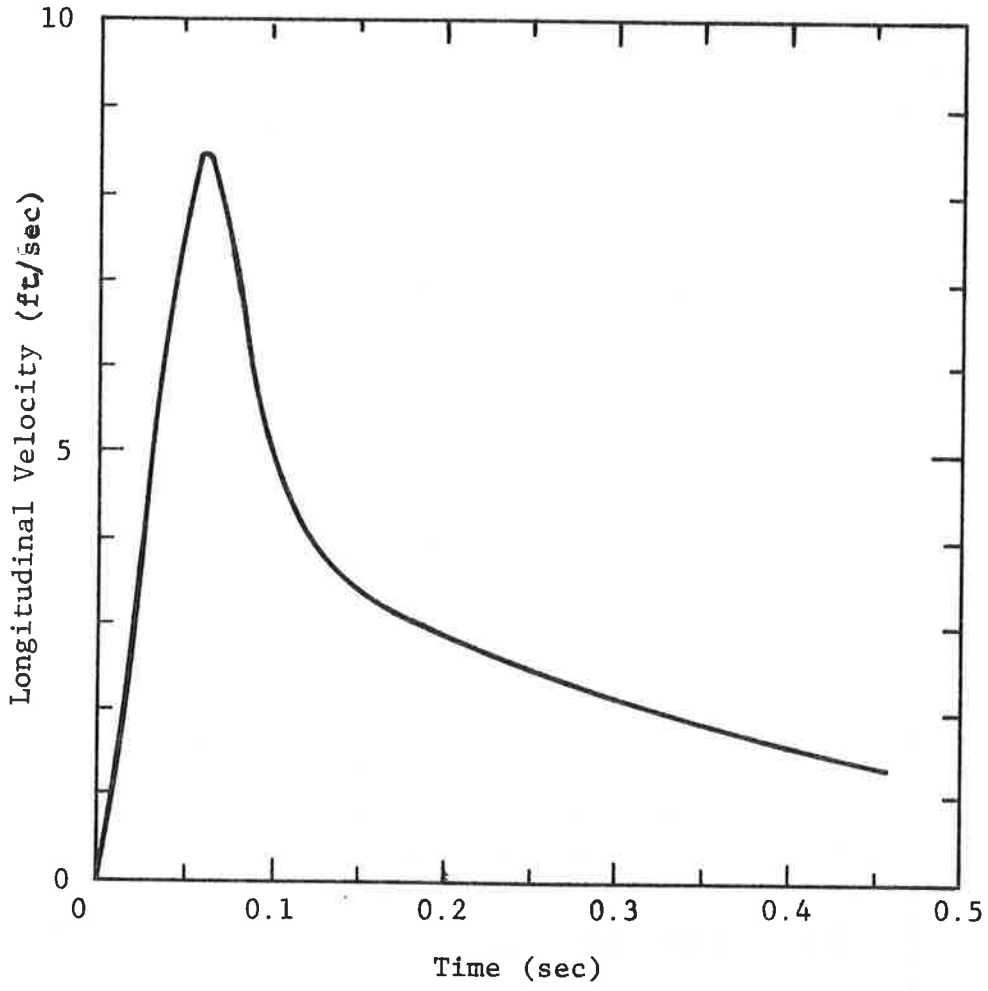

Figure 25. LONGITUDINAL VELOCITY OF STRUCK CAR ON ANVIL CAR TEST, 7.04 MPH IMPACT SPEED

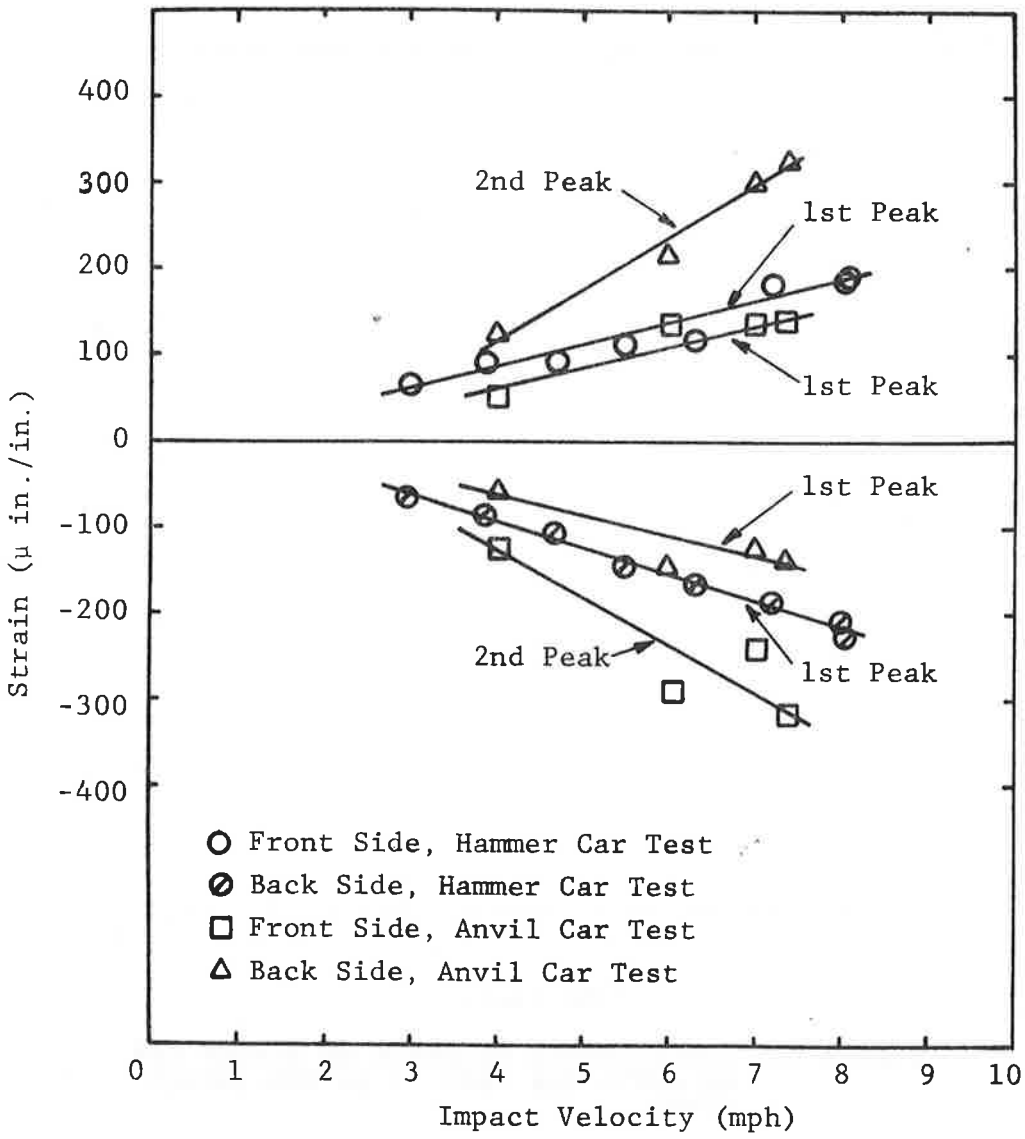

Figure 26. HORIZONTAL STRAINS MEASURED ON GAGES AT CENTER OF SHIELD, COMPARISON OF HAMMER CAR AND ANVIL CAR TEST DATA

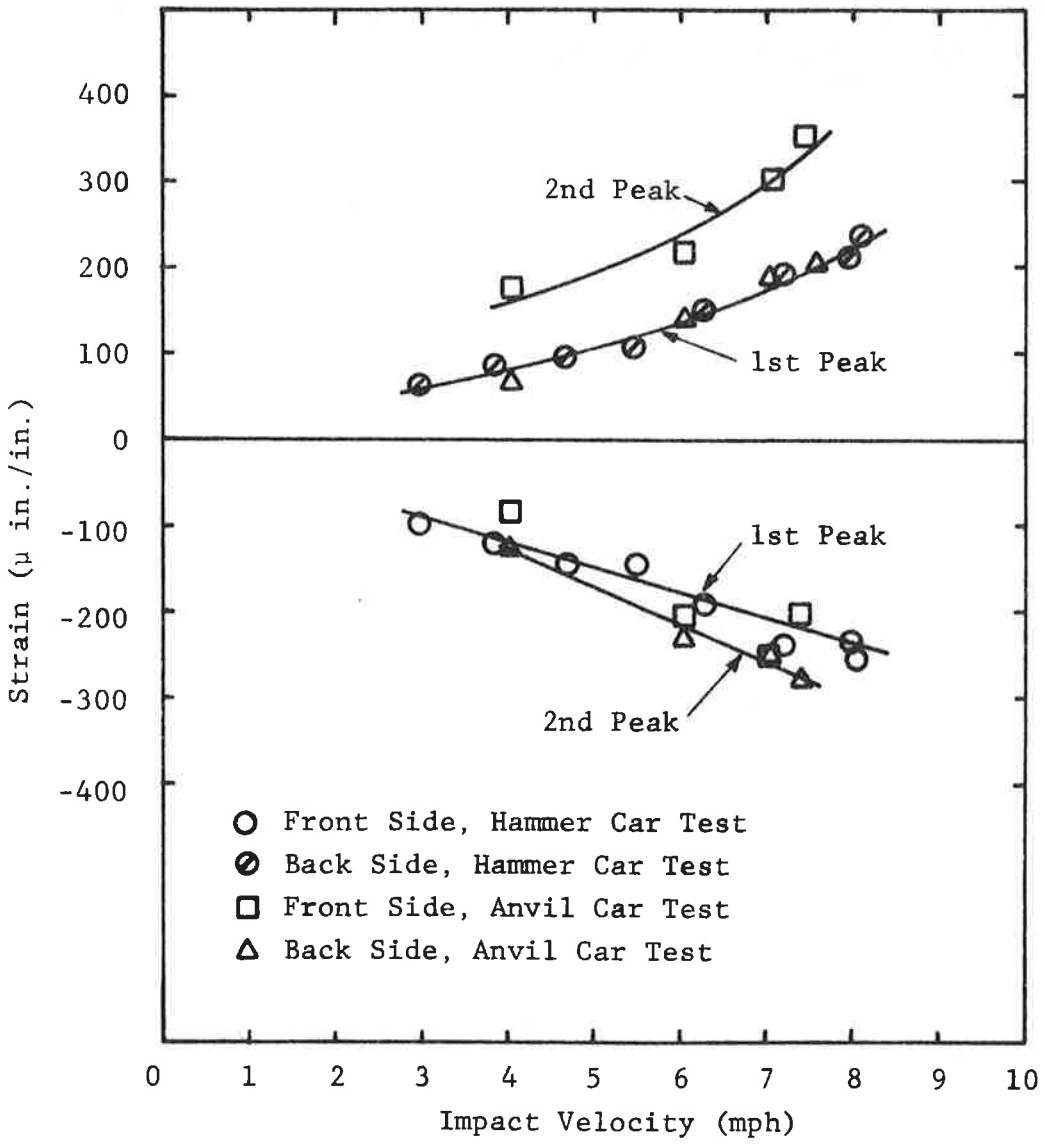

Figure 27. HORIZONTAL STRAINS MEASURED ON LEFT SIDE OF SHIELD, COMPARISON OF HAMMER CAR AND ANVIL CAR TEST DATA

Data from the strain gages on the support angle showed that the gages were strained beyond the yield point. This was the result of the severe vertical oscillations of the shield, which, as noted on the earlier tests, involved coupling of the longitudinal displacement into a complex vertical vibration. This caused the support angle to be alternately lifted off the stub sill and impacted downward on it.

4. CONCLUSIONS AND RECOMMENDATIONS

The test results confirm the original assumption that car coupling impacts are a severe environment for consideration in tank car head shield design and evaluation. The two versions of the prototype LTU shield examined in these tests withstood a total of 30 car coupling impacts with no apparent damage to the shield or its supporting structure, except for a small amount of inelastic deformation in the angle supporting the shield. The shield with the tube side supports deflected less in response to the inertial loads associated with the car impact than the shield with the more flexible strap side supports. From the limited comparative data obtained thus far it would appear that reducing the dynamic response is a desirable characteristic of shield design because it lessens the probability of coupling primary response motions into undesirable modes of vibration which lead to highly stressed components.

The forces transmitted to the tank car bolster through the side supports were less with the flexible strap side support than with the more rigid tube support. Although a fatigue evaluation of the side support connection to the bolster has not yet been completed, it is believed that a reliable connection can be designed to carry the forces transmitted by either type of support. The strains measured in the shield plate were lower with the flexible side supports than with the rigid side supports, but in all cases they were substantially below the yield strength of the material.

The most undesirable characteristic of the shield design was the behavior of the horizontal support angle. The inertial loads associated with car impact are primarily longitudinal, but the longitudinal displacements of the shield in response to this load were rapidly coupled into vertical vibrations. As described elsewhere in this report, this results in stresses within the angle sufficient to cause yielding and the impact of the angle against the stub sill. Although a detailed fatigue evaluation of the behavior of the angle and its effect on the side sills and stub

sill has not yet been performed, it is obvious that this characteristic of the present design is not acceptable from the standpoint of long-life reliability.

The large displacements and stresses measured in both the shield and its supporting structure during the anvil car impact tests emphasizes the importance of considering the dynamic motions associated with car accelerations in the prediction of shield response. Further efforts to develop satisfactory analytical means of predicting shield response under various impact conditions are recommended.

The next step in the evaluation of the prototype head shield is to examine its behavior under over-the-road conditions. The particular factors of concern in these tests will be to determine if vibrations of the car can be coupled into undesirable high amplitude vibrations of the shield which would lead to high stresses in the supporting structure. However, it is recommended that before these tests are conducted the present design of the shield be modified to minimize the undesirable dynamic behavior which leads to the high stresses in the support angle. One possible modification would be to firmly attach the angle to the stub sill. It is recommended that the impact tests be repeated following this modification to verify the improved performance of the design before beginning the over-the-road tests.

APPENDIX A

DESCRIPTION OF INSTRUMENTATION

Gage Channel No. (Note 1)	Transducer Description	Location	Recorder No. (Note 2)	Calibration Procedure (Note 3)
	Accelerometers (Natural Frequency) Triaxial Accelerometer (CEC 4-204-0012)	Upper Left Corner of Shield (see Fig. 6)		
1	50g Long. (880 Hz)		1	2g Static; 10g Shake Table
2	15g Lat. (530 Hz)		1	
3	15g Vert. (530 Hz)		1	
4	Long. Accel. (Columbia Res. Corp. Model 300, 3000 Hz)	Upper Right Corner of Shield	1	Post Test Ballistic Pendulum
5	Vert. Accel. (same as above)			
6	Long. Accel. (Statham A5-600-350, 1000 Hz)	Stub Sill, Behind Shield (see Figs. 6 and 7)	1	
7	Long. Accel. (Columbia Res. Corp. Model 300, 3000 Hz)		1	
8	Vert. Accel. (same as above)		1	
	Strain Rosette (Micro-measurement EA-06-125RD-350)	Upper Left Corner of Shield (see Fig. 6):		
9,10,11		Front Side	2	
12,13,14		Back Side	2	
	Four Strain Gages, Two Each Wired into a Bridge Sensitive to Bending Moment (Micro-measurement WK-06-250BG-350)	Strap Spring at Lowest Position (see Fig. 7)		Longitudinal Load at Strap Spring Shield Connection
15	See Note 4	Left Side	2	
16		Right Side	3	

Gage Channel No. (Note 1)	Transducer Description	Location	Recorder No. (Note 2)	Calibration Procedure (Note 3)
	Same as Nos. 15 and 16	Strap Spring Near Connection to Shield (see Fig. 7)		Longitudinal Load at Strap Spring Shield Connection
17		Left Side	2	
18		Right Side	3	
	Four Strain Gages	Support Angle Left Side (see Fig. 8)		
19	Two Each Wired into Separate Bridges Sensitive to Bending Moment	Adjacent to Side	2	Vertical Load
20		Sill	2	
21		Adjacent to Shield Support	2	
22			2	
		Support Angle Right Side (see Fig. 9)		
23	Same as Nos. 19-22	Adjacent to Side	3	
24		Sill	3	
25		Adjacent to Shield Support	3	
26			3	
27	Two Strain Gages Wired into A Bridge Sensitive to Bending Moment	Support Angle at Right of Stub Sill (see Fig. 10)	3	

Gage Channel No. (Note 1)	Transducer Description	Location	Recorder No. (Note 2)	Calibration Procedure (Note 3)
28 29	Two Strain Gages, One on the Front Side of the Plate and the other on the Rear Side of the Plate Oriented Horizontally (Micro-measurement EA-06-250 BF-350)	Near Center of the Shield (see Fig. 6)	2 2	
30	Displacement (Celesco PT-101-15A, 15 in. Travel)	Between Top of Shield and Tank Head (see Figs. 6 and 7)	3	Displace Cable Lead
31	Load Cell (Houston Scientific 2000-5.5)	Between Support Angle and Stub Sill	3	Load Test Machine
32	Dynamometer Coupler	Anvil Car (Hammer Car for AAR 24-5 Test)	2	Load Test Machine

Note 1: Gage Channel Nos. 2 through 8 and 31 discontinued after first test series

Note 2: Recorder No. 1: IITRI Ampex AR-200 mounted on tank car

Recorder No. 2: Miner Bell and Howell CPR-4010 located adjacent to test track

Recorder No. 3: IITRI Ampex FR-1300 located adjacent to test track

Note 3: Strain gage channel data were interpreted using the gage factor to calculate strains with reference to an electrical calibration signal

Note 4: For tests with tube supports gage Nos. 15-18 refer to individual strain gages placed on the tubes in the longitudinal direction at the center of the tube

APPENDIX B

REPORT OF INVENTIONS

After a diligent review of the work performed under this contract, no innovation, discovery, improvement or invention was made.